Computers & Operations Research 144 (2022) 105819

Contents lists available at ScienceDirect

Computers and Operations Research

journal homepage: www.elsevier.com/locate/cor

Constrained shortest path tour problem: Branch-and-Price algorithm

Sébastien Martin, Youcef Magnouche *, Corentin Juvigny, Jérémie Leguay

Huawei Technologies, France Research Center, 18 Quai du Point du Jour, 92100 Boulogne-Billancourt, France

ARTICLE INFO

Keywords:
Shortest path tour
Complexity
Integer linear programming
Integral polytope
Column generation
Dantzig–Wolfe decomposition

ABSTRACT

The constrained shortest path tour problem consists, given a directed graph $G = (V \cup \{s,t\}, A)$, an ordered set of disjoint vertex subsets $\mathcal{T} = \{T_1, \dots, T_k\}$ and a length function $c : A \to \mathbb{R}^+$, in finding a path between s and t of minimum length in G intersecting every subset of $\mathcal{T}$ in the given order such that each arc is visited at most once. In this paper, we first show that this problem is NP-Hard even in the most particular case when $\mathcal{T}$ contains only one subset with a unique vertex. Then, we introduce a new mathematical model for the problem that helps its decomposition and develop an efficient Branch-and-Price algorithm. We demonstrate that it can easily be applied to several problem variants. Finally, we present extensive computational results with a benchmark against the state of the art Branch-and-Bound algorithm, called $B\&B^{new}$, from Ferone et al. (2020). On a diverse set of instances, we show that our algorithm significantly decreases the worst computational time while the ranking of algorithms for the average varies over instances.

1. Introduction

The shortest path problem is a well-known optimization problem that has been studied extensively for decades (Taccari, 2016). Dijkstra or Bellman–Ford algorithms can solve it in polynomial time when there is no negative weights or negative cycles. However, for some applications, finding the shortest path is not enough. In particular, it is sometimes necessary to go through compulsory vertices or arcs in a given order before reaching the destination. In telecommunication networks for instance packets must be routed through a sequence of gateways or switches thanks to a mechanism called service function chaining (Bhamare et al., 2016a). If an arc can be visited multiple times, this problem can easily be reduced to solving the shortest path problem in a layered graph (Dwaraki and Wolf, 2016). However, in some cases, where we need to avoid routing loops, every arc must be visited at most once. In this case, the associated Constrained Shortest Path with Node Inclusions (CSPNI) problem becomes NP-Hard. This problem can be compared to the sequential ordering problem, a version of the traveling salesman problem with precedence relationships. Some algorithms, like a Lagrangian relax-and-cut approach (Escudero et al., 1994), and heuristic manipulation techniques (Montemanni et al., 2008) exist to solve it. In practice, each intermediate node to visit (e.g., the node hosting a network function in a telecommunication network) may not be exactly determined beforehand and, instead, a set of candidate nodes may be given for each inclusion. To handle sets of inclusion nodes, a more general problem, called the shortest path tour problem (SPTP), must be solved.

The Shortest Path Tour Problem (Festa et al., 2013) consists in finding the shortest path from an origin to a destination vertex such that the path must visit a sequence of non-empty disjoint vertex subsets $T_1, \dots, T_k$ in the order. The subsets are disjoints and may be of different sizes. In the Constrained Shortest Path Tour Problem (CSPTP) (Ferone et al., 2016), it is required, in addition, that the path does not include repeated arcs. This problem belongs to the complexity class of NP-complete problems. A Branch & Bound (B&B) and GRASP algorithms have also been proposed (Ferone et al., 2016) in 2016. The same authors have improved the model and the Branch & Bound algorithm, called $B\&B^{new}$, in 2020 (Ferone et al., 2020). Valid inequalities for the problem have been proposed in de Andrade and Saraiva (2018). In Saraiva and de Andrade (2021) authors develop Lagrangian-based heuristic for the problem. Recent extensions of the problem such as the Constrained Forward Shortest Path Tour Problem (CFSPTP) have been studied (Carrabs et al., 2020). In this variant, the path can cross a subset of vertices only if all previous subsets are already visited. For instance, the path crossing the subsets T_1, T_3, T_2, T_3 in this order, is not feasible for CFSPTP since T_3 is visited before T_2. However this path remains feasible for CSPTP since T_2 is visited after T_1 and T_3 is visited after T_2. In Sasabe and Hara (2021), the authors study a variant for telecommunication networks where the shortest path tour and inclusion node placement are considered jointly. They show a graph transformation to consider node placement in the shortest path tour problem under link and node capacity constraints. According to this transformation they propose an integer linear program. Another

* Corresponding author.
E-mail address: youcef.magnouche@huawei.com (Y. Magnouche).

https://doi.org/10.1016/j.cor.2022.105819
Received 14 September 2021; Received in revised form 28 March 2022; Accepted 28 March 2022
Available online 7 April 2022

variant of the SPTP considering time windows has been studied in Di Puglia Pugliese et al. (2020).

In this paper, we focus on the CSPTP problem and we show that our results can easily be extended for other variants like CFSPTP.

As mentioned before, one of the main applications of the shortest path tour problem belongs to the telecommunication domain. Thanks to the advent of software virtualization, network operators are now deploying network functions (e.g., firewalls, media gateways) as virtual machines to replace physical devices. The virtualization of network functions allows the use of commodity servers to host them. This makes network services highly scalable as virtual machines can simply be replicated to follow a growing traffic demand. This trend is strongly supported by Internet service providers (ISPs) (Mijumbi et al., 2016) to build the so-called Network Function Virtualization (NFV) infrastructure. In this context, a major challenge is to deploy Service Function Chains (SFC) (Bhamare et al., 2016b) where traffic from a customer has to traverse a set of network functions in a given order. While the operator defines the type of each function, the exact virtual instance traversed by a given flow can be determined automatically to optimize the use of resources. In such a case, the shortest path, which crosses, in order, each set of network function instances, must be calculated.

This paper makes the following contributions:

- Complexity results: we prove that the CSPTP is NP-Hard even in the most particular case when only one subset of size 1 is considered and the path must be simple (an arc cannot be crossed twice) or elementary (a vertex cannot be crossed twice). We also show that CSPTP is polynomial in DAGs (Directed Acyclic Graphs).
- Branch-and-Price algorithm: we provide an extended model that eases the problem decomposition and design an efficient associated pricing problem and a branching scheme to find the optimal solution. We show that the algorithm can, easily, be adapted and applied to several variants of CSPTP.
- Experimental results: we compare our exact algorithm with the best exact algorithm from the state of the art (i.e., $B\&B^{new}$ algorithm from Ferone et al. (2020)). On a diverse set of instances, we show that our algorithm significantly decreases the worst computational time while the ranking of algorithms for the average varies over instances.

This paper is organized as follows. In Section 2, some definitions, used in the paper, are given. In Section 3, we present a complexity analysis for the variants of the CSPTP. Then, we give a compact model in Section 4 and an extended model in Section 5 for the problem. In Section 6 we explain how the Branch-and-Price algorithm can be adapted to other CSPTP variants. Finally, in Section 7, we present and discuss some numerical results.

2. Definitions and problem description

In this section, we present the CSPTP problem and some basic definitions. Let $G = (V \cup \{s,t\}, A)$ be a directed graph where V is the set of vertices, A is the set of arcs and s,t are two particular vertices corresponding to a source and a destination. Function $c : A \to \mathbb{R}^+$ assigns a distance $c_{(u,v)}$ to each arc $(u,v) \in A$. For every vertex $v \in V$, let $\delta^+(v)$ and $\delta^-(v)$ be the set of egress and ingress arcs of v, respectively.

A path $p = \{v_0, \dots, v_{|p|}\}$ is a sequence of vertices, such that $(v_i, v_{i+1}) \in A$, for all $i \in \{0, \dots, |P|-1\}$. We denote by $A(p) = \{(v_i, v_{i+1}) : i \in \{0, \dots, |P|-1\}\}$ the set of arcs in the path p. A path is said to be *simple* (resp. elementary) if no arc (resp. vertex) is repeated in it.

We denote by $\mathcal{T} = \{T_1, \dots, T_k\}$ an ordered set of *inclusion subsets* where $T_i \subset V$, for $i \in \{1, \dots, k\}$ and $T_i \cap T_j = \emptyset$ for all $i, j \in \{1, \dots, k\}$ with $i \neq j$. In the following we can denote $T_0 = \{s\}$ and $T_{k+1} = \{t\}$.

A path p is called a *path tour* of $\mathcal{T} = \{T_1, \dots, T_k\}$ if it exists a subset of vertices $I = \{v_1^I, \dots, v_k^I\}$ such that $v_i^I \in T_i$ for $i \in \{1, \dots, k\}$ and p visits each vertex of I respecting the order. For instance, on Fig. 1 the path in (bold dashed line) crosses several times each subset (T_1, T_3, T_2, T_1, T_3). This path is valid since by selecting the vertices c, e, h the order of $\mathcal{T}$ is respected. The Constrained Shortest Path Tour Problem (CSPTP) consists in finding a simple shortest path p from s to t of minimum length. This path is said to be valid for $\mathcal{T}$.

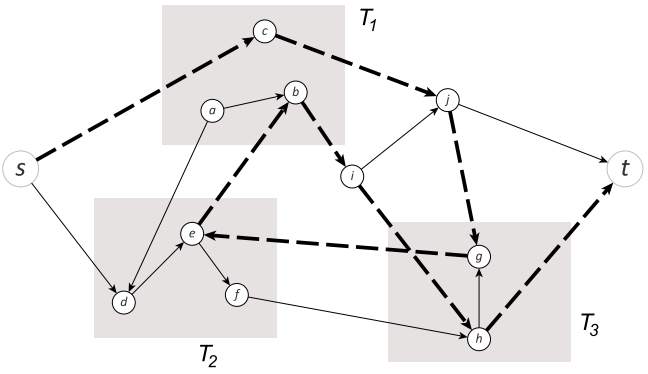

Fig. 1. Shortest path tour example (bold dashed line) from s to t with 3 inclusion subsets (i.e., T_1, T_2 and T_3).

In the next section, we discuss the complexity of the Constrained Shortest Path Tour Problem (CSPTP).

3. Complexity analysis

The constrained shortest path tour problem is polynomial when $\mathcal{T} = \{\emptyset\}$ as it reduces to a shortest path problem, whose linearity is well known. In Ferone et al. (2016), Ferone et al. show that CSPTP is NP-Hard, in general. They show that the Hamiltonian Path Problem (Bertossi, 1981), known NP-Hard, can be polynomially reduced to the CSPTP. In the following, we focus on the most particular case of the CSPTP with one inclusion subset of size 1, i.e., $\mathcal{T} = \{\{v'\}\}$ and we show that it is still NP-Hard. We also extend the result to consider the case of elementary paths. We also show that CSPTP is polynomial in DAGs (Directed Acyclic Graphs).

We denote by D-CSPTP the decision problem associated with the CSPTP that consists in checking if a valid path tour exists for $\mathcal{T}$ or not. Let us remark that for the decision problem the objective function is not needed.

Theorem 1. *D-CSPTP is NP-Complete if* $\mathcal{T} = \{\{v'\}\}$.

Proof. Clearly, the problem is in NP, since checking if a sequence of arcs is a simple path can be done in polynomial time. The following proof consists of a polynomial reduction from the directed two-commodity integral flow problem (2CIFP) with unit capacities to the constrained shortest path tour problem with a single inclusion subset of size 1. The 2CIFP with unit capacities is an NP-complete problem (Garey and Johnson, 1979) that consists, given a directed graph $G = (V, A)$ in computing a path p_1 from $s_1 \in V$ to $t_1 \in V$ and a path p_2 from $s_2 \in V$ to $t_2 \in V$ such that each arc belongs to at most one path, i.e., $A(p_1) \cap A(p_2) = \emptyset$. The problem reduction consists in constructing a new graph $\bar{G} = (\bar{V} \cup \{s_1, t_2\}, \bar{A})$ by adding vertex v' and two arcs (t_1, v') and (v', s_2), i.e. $\bar{V} = V \cup \{t_1, s_2, v'\}$ and $\bar{A} = A \cup \{(t_1, v'), (v', s_2)\}$, where $\mathcal{T} = \{\{v'\}\}$. Fig. 2 illustrates the graph transformation where Fig. 2(a) represents graph G and Fig. 2(b) represents graph $\bar{G}$.

Therefore if there exists a valid path between s_1 and t_2 for $\mathcal{T} = \{\{v'\}\}$ in $\bar{G}$, then the associated flow f_1 between s_1 and t_1 and the associated flow f_2 between s_2 and t_2 are valid for the 2CIFP. Furthermore, if there does not exist a simple path tour between s_1 to t_2 in $\bar{G}$, there cannot exist two flows f_1 and f_2 in G. □

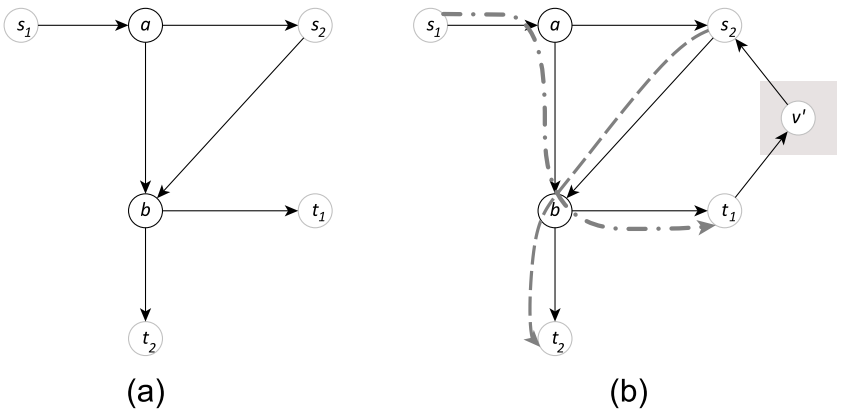

Fig. 2. Problem reduction from 2CIFP to CSPTP with $\mathcal{T} = \{\{v'\}\}$.

Corollary 1. *CSPTP is strongly NP-Hard.*

Let us denote by CSPTP-E the variant where the path must be elementary, i.e. every vertex cannot be visited more than once. As we can split each vertex into two vertices connected by an arc, CSPTP is more generic than CSPTP-E. Therefore, solving CSPTP-E in the original graph is equivalent to solving the CSPTP in the new graph. We denote by D-CSPTP-E the decision problem of CSPTP-E. We will show that this problem is still NP-Hard in the simple case where $\mathcal{T} = \{\{v'\}\}$.

Theorem 2. *D-CSPTP-E is NP-Complete if* $\mathcal{T} = \{\{v'\}\}$.

Proof. In the following, we propose a polynomial reduction from D-CSPTP to D-CSPTP-E. From Theorem 1, the D-CSPTP is NP-complete. Let $G = (V \cup \{s,t\}, A)$ and $\mathcal{T} = \{\{v'\}\}$ be an instance of D-CSPTP. Let $\bar{G} = (\bar{V} \cup \{s,t\}, \bar{A})$ be the graph obtained from G as follows

1- add vertices $\bar{s}$, $\bar{t}$ and $\bar{v}'$ to $\bar{V}$.
2- for every vertex $u \in V \cup \{s,t\}$, for all $a \in (\delta^+(u) \cup \delta^-(u))$ add a vertex u_a to $\bar{V}$.
3- for every vertex $u \in V \cup \{s,t\}$, add an arc to $\bar{A}$ between every pair of vertices in $K_u = \{u_a \mid a \in (\delta^+(u) \cup \delta^-(u))\}$ in order to obtain a clique. K_u is called a *clique of* u.
4- for every arc $(u,v) \in A$, add an arc to $\bar{A}$, between $u_{(u,v)}$ and $v_{(u,v)}$.
5- add an arc between $\bar{s}$ and each vertex s_a where $a \in \delta^+(s)$.
6- add an arc between each vertex t_a and $\bar{t}$ where $a \in \delta^-(t)$.
7- add an arc between $\bar{v}'$ and each vertex v'_a where $a \in \delta^+(v')$.
8- add an arc between each vertex v'_a and $\bar{v}'$ where $a \in \delta^-(v')$.

Fig. 3 illustrates the above transformation on the example given in Fig. 2(b).

Claim 1. *There exists an elementary path* $\bar{p}$ *valid for* $\mathcal{T} = \{\{\bar{v}'\}\}$ *in* $\bar{G}$ *iff there exists a simple path* p *in* G *crossing* v'.

Proof. ($\Rightarrow$) Let $p = \{s, u^1, u^2, \dots, u^l, v', w^1, w^2, \dots, w^m, t\}$ To simplify the notation s is called u^0, t is called w^{m+1} and v' is called u^{l+1} or w^0. Path $\bar{p}$ is given by the following arcs:

- $(\bar{s}, u^0_{(u^0,u^1)})$, $(u^{l+1}_{(u^l,u^{l+1})}, \bar{v}')$, $(\bar{v}', w^0_{(w^0,w^1)})$, $(w^{m+1}_{(w^m,w^{m+1})}, \bar{t})$,
- $(u^i_{(u^{i-1},u^i)}, u^i_{(u^i,u^{i+1})})$, for each $i \in \{1, \dots, l\}$,
- $(u^i_{(u^i,u^j)}, u^j_{(u^i,u^j)})$, for each $(u^i, u^j) \in p$,
- $(w^i_{(w^{i-1},w^i)}, w^i_{(w^i,w^{i+1})})$, for each $i \in \{1, \dots, m\}$,
- $(w^i_{(w^i,w^j)}, w^j_{(w^i,w^j)})$, for each $(w^i, w^j) \in p$.

We obtain the following path $\bar{p} = \{\bar{s}, u^0_{(u^0,u^1)}, u^1_{(u^0,u^1)}, u^1_{(u^1,u^2)}, \dots, u^{l+1}_{(u^l,u^{l+1})}, \bar{v}', w^0_{(w^0,w^1)}, w^1_{(w^0,w^1)}, w^1_{(w^1,w^2)}, \dots, w^{m+1}_{(w^m,w^{m+1})}, \bar{t}\}$. Since path p is a simple path, an arc is not visited twice as vertices of $\bar{p}$ are indexed by arcs. It follows that path $\bar{p}$ visits each vertex at most once and the path $\bar{p}$ is elementary.

($\Leftarrow$) Let $\bar{p}$ be the path between $\bar{s}$ and $\bar{t}$ in $\bar{G}$. Path p can be obtained from $\bar{p}$, by removing the arcs of all cliques of all vertices, and replacing

- arc $(\bar{s}, u^0_{(u^0,u^1)})$ by arc (s, u^1),
- arc $(u^i_{(u^i,u^j)}, u^j_{(u^i,u^j)})$ by arc (u^i, u^j),
- arc $(u^{l+1}_{(u^l,u^{l+1})}, \bar{v}')$ by arc (u^l, v'),
- arc $(\bar{v}', w^0_{(w^0,w^1)})$ by arc (v', w^1),
- arc $(w^i_{(w^i,w^j)}, w^j_{(w^i,w^j)})$ by arc (w^i, w^j),
- arc $(w^{m+1}_{(w^m,w^{m+1})}, \bar{t})$ by arc (w^m, t).

Then, we obtain path $p = \{s, u^1, \dots, u^l, v', w^1, \dots, w^m, t\}$. Since path $\bar{p}$ is elementary, it follows that paths p is simple. □

From Claim 1, finding an elementary path in $\bar{G}$ is equivalent to finding a simple path in G. Since the CSPTP is NP-complete, the CSPTP-E so is. □

Corollary 2. *CSPTP-E is strongly NP-Hard.*

Proposition 1. *The CSPTP is polynomial in DAGs (Directed Acyclic Graphs).*

Proof. Let $\mathcal{T} = \{T_1, \dots, T_k\}$ be the set inclusion subsets. Let $H = (V' \cup \{s,t\}, A')$ be a directed acyclic graph such that

- V' contains k copies of V indexed by i, i.e., $(v^1, v^2, \dots, v^k)$
- A' contains k copies of A indexed by i, i.e., for $a = (u,v)$ in A we obtain $a^i = (u^i, v^i)$ for $i \in \{1, \dots, k\}$
- for each $i \in \{1, \dots, k\}$, $u \in T_i$, $(u,v) \in \delta^+(u)$ add an arc (u^i, v^{i+1}) to A'
- for all $(s,v) \in \delta^+(s)$, add (s, v^1) to A'
- for all $(v,t) \in \delta^-(t)$, add (v^k, t) to A'

The shortest path $\bar{p}$ between s and t in H where the indices are deleted is a valid path p for $\mathcal{T}$ in G. Indeed, if u^i belongs to $\bar{p}$ then u belongs to p. As G is a DAG then no arc can be crossed twice in p. □

4. Compact formulation for CSPTP

In Ferone et al. (2020), Ferone et al. have presented a compact formulation for the CSPTP which aims at constructing a set I that contains one selected vertex for every inclusion subset of $\mathcal{T}$, and computing a simple path that crosses over all vertices of I in the order.

This model requires two types of integer variables

$$x^i_a = \begin{cases} 1 & \text{if } a \text{ belongs to the path between} \\ & \quad T_i \text{ and } T_{i+1}. \\ 0 & \text{otherwise.} \end{cases} \qquad \forall\, a \in A,\ i \in \{0, ..., k\}.$$

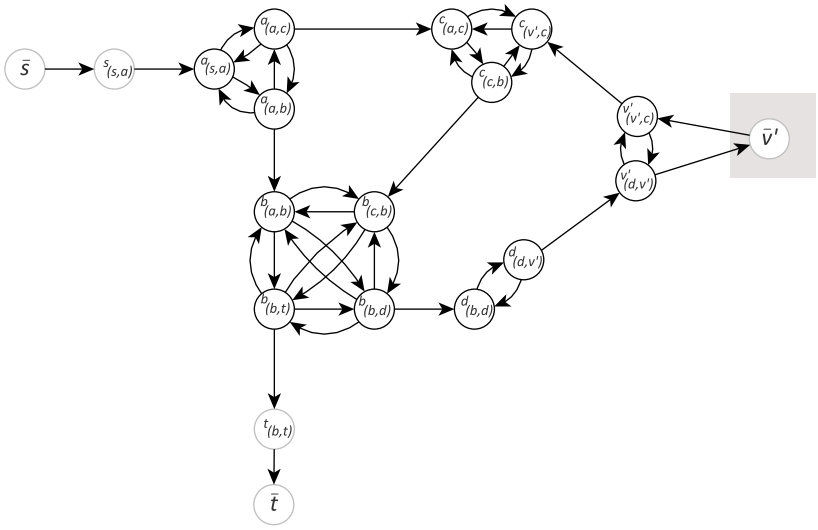

Fig. 3. Illustration of the graph transformation of G with $\mathcal{T} = \{\{v'\}\}$ to $\bar{G}$ with $\mathcal{T} = \{\{\bar{v}'\}\}$ for CSPTP-E.

$$y_v = \begin{cases} 1 & \text{if } v \text{ is one of selected inclusion} \\ & \quad \text{vertices } (v \in I). \\ 0 & \text{otherwise.} \end{cases} \qquad \forall v \in V_i,\ i \in \{1, ..., k\}.$$

The constrained shortest path tour problem is equivalent to the following integer linear program:

$$\min \sum_{i\in\{0,\dots,k\}} \sum_{a\in A} c_a x_a^i \tag{1}$$

$$\text{s.t.} \sum_{a\in\delta^+(v)} x_a^i - \sum_{a\in\delta^-(v)} x_a^i = \begin{cases} y_v & \text{if } v \in T_i \\ -y_v & \text{if } v \in T_{i+1} \\ 0 & \text{otherwise.} \end{cases} \qquad \forall v \in V,\ \forall i \in \{0, \dots, k\}, \tag{2}$$

$$\sum_{i\in\{0,\dots,k\}} x_a^i \le 1 \qquad \forall a \in A, \tag{3}$$

$$\sum_{v\in T_i} y_v = 1 \qquad \forall i \in \{1, \dots, k\}, \tag{4}$$

$$y_s = y_t = 1 \tag{5}$$

$$x_a^i \in \{0, 1\} \qquad \forall a \in A,\ \forall i \in \{0, \dots, k\}, \tag{6}$$

$$y_v \in \{0, 1\} \qquad \forall v \in T_i, \forall i \in \{1, \dots, k\}. \tag{7}$$

where Constraints (2) represent the flow conservation constraints between each consecutive successive pair of inclusion vertices in I, ensuring a path between consecutive inclusion vertices. Constraints (3) guarantee that every arc is visited at most once and Constraints (4)–(5) ensure that exactly one vertex is selected from every subset of $\mathcal{T}$, ensuring the selection of one inclusion vertex in each subset of $\mathcal{T}$. Based on the idea of this model, the authors proposed the $B\&B^{new}$ algorithm. While the mathematical model is not used in $B\&B^{new}$, the considered branching rules forbid links between consecutive inclusion vertices. The goal at each node of the branching tree is to compute shortest paths between every possible couple of consecutive inclusion vertices according to the forbidden links. A dynamic programming algorithm is proposed to find the shortest sequence of paths within the pool of all generated paths respecting the current forbidden rules. If there exists a feasible sequence of shortest paths, then the solution is used to update the bound, otherwise there exists at least one link belonging to multiple paths. In this case, branching nodes are generated to forbid this link to be selected.

In this section, we introduce a new compact model based on a graph transformation, leading to only one type of variables. Let $\bar{G} = (\bar{V} \cup \{s, t\}, \bar{A})$ be the graph obtained from G by adding a dummy vertex v_i to $\bar{V}$ and two arcs (v, v_i) and (v_i, v) to $\bar{A}$ for each vertex $v \in T_i$ and for all $T_i \in \mathcal{T}$. All new arcs have a length 0. Fig. 4 illustrates the graph transformation on the example given in Fig. 1.

Solving the CSPTP with $\mathcal{T} = \{\{v_1\}, \dots, \{v_k\}\}$ in $\bar{G}$ does not always give a feasible solution in G. Indeed on Fig. 4, the path $\{s, b, v_1, a, d, v_2, d, e, f, v_3, f, t\}$ is not a valid path tour for G. Therefore, incompatibility constraints are required to ensure that arc (v, v_i) belongs to the path if and only if (v_i, v) belongs also to the path. In the following, for the sake of clarity, let denote by v_0 vertex s and by v_{k+1} vertex t.

Let $x \in \{0, 1\}^{|\bar{A}|\times k}$ be a variable vector such that x_a^i equals 1 if a belongs to the sub-path between v_i and v_{i+1}, and 0 otherwise, for all $i \in \{0, \dots, k\}$. The constrained shortest path tour problem is equivalent to the following integer linear program CSPTP-IP based on the extended graph $\bar{G}$:

$$\min \sum_{i=0}^{k} \sum_{a\in\bar{A}} c_a x_a^i \tag{8}$$

$$\sum_{a\in\delta^+(v)} x_a^i - \sum_{a\in\delta^-(v)} x_a^i = \begin{cases} 1 & \text{if } v = v_i \\ -1 & \text{if } v = v_{i+1} \\ 0 & \text{otherwise.} \end{cases} \qquad \forall v \in \bar{V},\ \forall i \in \{0, \dots, k\}, \tag{9}$$

$$\sum_{i=0}^{k} x_a^i \le 1 \qquad \forall a \in \bar{A}, \tag{10}$$

$$x_{(v,v_i)}^{i-1} + \sum_{v'\in T_i\setminus\{v\}} x_{(v_i,v')}^i \le 1 \qquad \forall v \in T_i, \forall i \in \{1, \dots, k\}, \tag{11}$$

$$x_{(v,v_i)}^j = 0 \qquad \forall v \in T_i, \forall i, j \in \{0, \dots, k\}, (i-1) \ne j, i \ge 1, \tag{12}$$

$$x_{(v_i,v)}^j = 0 \qquad \forall v \in T_i, \forall i, j \in \{0, \dots, k\}, i \ne j, i \ge 1, \tag{13}$$

$$x_a^i \in \{0, 1\} \qquad \forall a \in \bar{A},\ \forall i \in \{0, \dots, k\}. \tag{14}$$

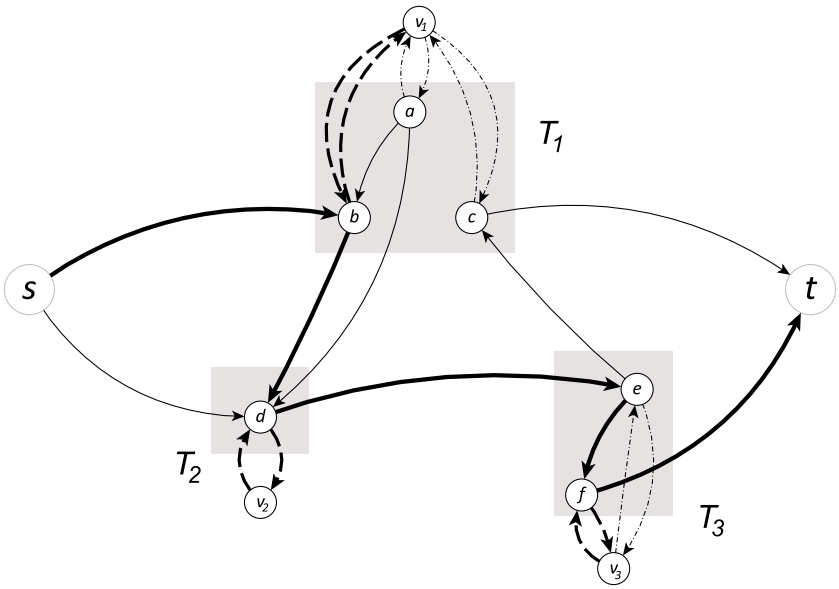

Fig. 4. Illustration of the graph transformation for a shortest path tour (bold line) between s and t and with 3 inclusion subsets (i.e., T_1, T_2 and T_3).

where Constraints (9) represent the flow conservation constraints required between dummy vertices according to the graph transformation. Constraints (10) guarantee that every arc is visited at most once. Constraints (12) and (13) ensure that the dummy arcs are used in the right sub-path. Constraints (11) guarantee that if a vertex of T_i, for $i \in \{1, \dots, k\}$, is used to go directly to v_i then the same vertex is used to go back from v_i. These constraints ensure the selection of only one vertex for each set $\mathcal{T}$ according to the graph transformation. The graph transformation allows to remove the second set of variables by adding additional vertices and arcs. While the two models are similar, the latter has a better structure for decomposition.

In the next section, we present an extended model based on the Dantzig–Wolf decomposition (Dantzig and Wolfe, 1960). This decomposition does not change the linear relaxation. However, it decreases the number of inequalities in the formulation and allows a dynamic variables generation (see next section).

5. Path formulation

In this section, we consider an extended model based on CSPTP-IP where each variable represents a sub-path in the graph $\bar{G}$. Remark that any feasible (valid) path p is composed of k sub-paths $p_0, \dots, p_k$. Let P_i be the set of all possibles simple paths between v_i and v_{i+1} in $\bar{G}$, for all $i \in \{0, \dots, k\}$, not crossing any other dummy vertex v_j, for all $j \in \{0, \dots, k\} \setminus \{i, i+1\}$. Let $P = \bigcup_{i=0}^{k} P_i$. Due to the Constraints (11) any concatenation of sub-paths may not be a feasible solution. Fig. 5 displays a graph with two inclusion subsets of size 1, i.e., $\mathcal{T} = \{\{c\}, \{e\}\}$. Each inclusion subset T_i is connected to one dummy node v_i as described in Section 4. The figure shows 3 sub-paths: one path between s and v_1, one path between v_1 and v_2 and one path between v_2 and t.

Let $\lambda \in \{0,1\}^{|P|}$ be a variable vector such that λ_p equals 1 if the sub-path $p \in P$ is selected and 0 otherwise. Note that variables λ are exponential in number.

The CSPTP-IP is equivalent to the following integer linear program called CSPTP-CG, that can be used for Column Generation (CG), in $\bar{G}$

$$\min \quad \sum_{i=0}^{k} \sum_{p \in P_i} \sum_{a \in p} c_a \lambda_p \tag{15}$$

$$\sum_{p \in P_i} \lambda_p = 1 \qquad \forall i \in \{0, \dots, k\}, \tag{16}$$

$$\sum_{i=0}^{k} \sum_{p \in P_i : a \in A(p)} \lambda_p \leq 1 \qquad \forall a \in \bar{A}, \tag{17}$$

$$\sum_{p \in P_{i-1} : (v, v_i) \in A(p)} \lambda_p + \sum_{p \in P_i : (v_i, v) \notin A(p)} \lambda_p \leq 1 \qquad \forall v \in T_i, i \in \{1, \dots, k\}, \tag{18}$$

$$\lambda_p \in \{0,1\} \qquad \forall p \in P_i, i \in \{0, \dots, k\}. \tag{19}$$

Constraints (16) represent the convexity constraints which ensure that only one sub-path is selected between each consecutive successive inclusion subsets. Capacity constraints are given by inequalities (17) ensuring that each arc is used at most once (related to Constraints (10)). Constraints (18) ensure that if (v, v_i) is in the path then (v_i, v) is also in the path, for all $i \in \{1, \dots, k\}$ (related to Constraints (11)). Constraints (19) impose the variables to be binary. By relaxing constraints (19), and replacing them by

$$\lambda_p \geq 0 \qquad \forall p \in P_i, i \in \{0, \dots, k\} \tag{20}$$

we obtain the linear relaxation of CSPTP-CG, denoted CSPTP-CG-R.

First, we present the two key ingredients of the Branch-and-Price algorithm, which are the pricing problem and the branching scheme. Then, we explain the Branch-and-Price algorithm that we develop on top of these two concepts.

5.1. Pricing problem

Solving CSPTP-CG-R can be efficiently achieved using the column generation method due to the exponential number of variables. It is equivalent to the cutting plane method in the dual problem. Each column in the primal problem has an associated constraint in the dual problem. At each iteration, CSPTP-CG-R is solved with a subset of columns, called *restricted master problem* and new columns are generated. The first restricted master problem is initialized with an artificial variable that appears in Constraints (16) with a high length in the objective function. This variable ensures the feasibility of the restricted master problem. The new columns, added at every iteration, are generated by solving the following pricing problem. This problem consists in finding a violated constraint in the dual. For all $i \in \{0, \dots, k\}$ and $p_i \in P_i$ the dual of path variable λ_p, is equivalent to the following

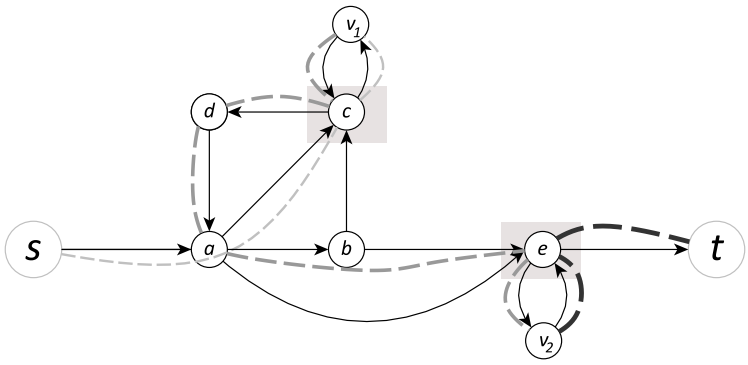

Fig. 5. Three sub-paths between s and t in dashed lines: from s to v_1 (light gray), from v_1 to v_2 (gray) and from v_2 and t (dark gray).

constraint:

$$\sum_{a\in A(p_i)}(c_a+\alpha_a)+\sum_{v\in T_{i+1}:v\in p_i}\theta_v^{i+1}+\sum_{v\in T_i:v\notin p_i}\theta_v^{i}\geq\beta_i \tag{21}$$

where β, α and θ represent the dual variables associated with the Constraints (16), (17) and (18), respectively. Let β^*, α^* and θ^* represent the current dual values associated with the Constraints (16), (17) and (18), respectively, of CSPTP-CG-R.

To solve the pricing problem, we simply need to find a path p_i with a shortest path algorithm between v_i and v_{i+1} for each $i \in \{0,\dots,k\}$ such that no vertex v_j, for all $j \in \{0,\dots,k\} \setminus \{i, i+1\}$ is crossed and $\sum_{a\in A(p_i)}(c_a+\alpha_a^*)+\sum_{v\in T_{i+1}:v\in p_i}\theta_v^{*i+1}+\sum_{v\in T_i:v\notin p_i}\theta_v^{*i}-\beta_i^*$ is minimum. If the value is negative then the column is added, as the associated dual constraint is violated. This is equivalent to solving the shortest path problem between v_i and v_{i+1} where the length of

- every arc $(u,v)\in A$ is $c_{(u,v)}+\alpha^*_{(u,v)}$,
- every arc (v_i,v) is $\sum_{v\in T_i\setminus\{v\}}\theta_v^{*i}$, for all $v\in T_i$,
- every arc (v,v_{i+1}) is θ_v^{*i+1}, for all $v\in T_{i+1}$,

in the graph obtained from $\bar{G}$ by removing all the ingress and egress arcs of every dummy vertex v_j for all $j \in \{0,\dots,k\}\setminus\{i,i+1\}$. If the length of path p_i is less than β_i^* thus the associated column is added.

Note that, as the pricing problem can be solved in a polynomial time, the CSPTP-CG-R so is.

5.2. Branching scheme

CSPTP-CG-R solves the linear relaxation of the CSPTP which may give a fractional solution. Therefore, it must be coupled with a Branch-and-Bound algorithm to ensure finding the optimal feasible integer solution. This latter is called a Branch-and-Price algorithm where CSPTP-CG-R is solved at every node of the branching tree.

In Barnhart et al. (2000), the authors proposed a branching scheme for the multi-commodity flow problem that consists, for a given commodity k, in finding two vertices u and v where the sum of paths, crossing both u and v, is fractional. The first branching node forbids all paths crossing u and the second one forbids all paths crossing v. The advantage of this branching scheme is that the constraints of the pricing problem do not change. It only filters all egress arcs of u or v from the graph. For CSPTP, we adapt this branching scheme and we derive two branching rules. Let λ^* be a fractional optimal solution (extreme point).

Branching rule 1:

- Case where there are two paths $p_i \in P_i$ and $p_j \in P_j$ for $i,j \in \{0,\dots,k\}$ with $i \neq j$ and one arc $a \in A$ in common between p_i and p_j, i.e., $a \in A(p_i)\cap A(p_j)$ such that $\lambda^*_{p_i}>0$ and $\lambda^*_{p_j}>0$. In this case, two branching nodes can be generated with the following constraints :

  (1) $\sum_{p\in P_i:a\in A(p)}\lambda_p^*=0$

  (2) $\sum_{l\in\{0,\dots,k\}\setminus\{i\}}\sum_{p\in P_l:a\in A(p)}\lambda_p^*=0$

Branching rule 2:

- Case where there are, for a given $i\in\{0,\dots,k\}$, two different sub-paths $p_1,p_2\in P_i$ and a dummy arc $a\in(\bar{A}\setminus A)$ such that $a\in A(p_1)$ and $a\notin A(p_2)$ and $0<\lambda^*_{p_1}<1$ and $0<\lambda^*_{p_2}<1$. Two branching nodes vertices can be generated with the following constraints :

  (1) $\sum_{p\in P_i:a\in A(p)}\lambda_p^*=0$

  (2) $\sum_{p\in P_i:a\notin A(p)}\lambda_p^*=0$

Remark that in each node of the branching tree, we filter the columns, of the restricted master problem, not satisfying the current branching constraints by setting the variable upper bound to 0.

Proposition 2. *Branching rules 1 and 2 applied in sequence provide a complete branching scheme for CSSPTP-CG.*

Proof. First, remark that branching rules 1 and 2 split the search area in two sub areas enumerating all possible solutions in the branching tree. Second, we show that each leaf of the branching tree provides an integer solution. Let l be a leaf of the branching tree (a node where the branching rules 1 and 2 cannot be applied). Let $P_0^{*l},\dots,P_k^{*l}$ be paths subsets such that $P_i^{*l}=\{p \mid \lambda_p^{*l}>0$ for all $p\in P_i\}$ for all $i\in\{0,\dots,k\}$. Since rule 1 cannot be applied, every paths $p_i\in P_i^{*l}$ and $p_j\in P_j^{*l}$, with $i\neq j$, cannot share any arc, i.e., $A(p_i)\cap A(p_j)=\emptyset$. Moreover, since rule 2 cannot be applied, each pair of paths $p_i^1,p_i^2\in P_i^{*l}$ has the same dummy arcs. Thus two paths $p_i^1,p_i^2\in P_i^*$ have the same cost, otherwise the solution is not optimal. Thus, an integer solution with the same objective value can be obtained by keeping only one path in each set of $P_0^{*l},\dots,P_k^{*l}$ and the proof is ended. □

5.3. Branch-and-Price algorithm

The overall Branch-and-Price algorithm consists in merging Branch-and-Bound and column generation algorithms to obtain an optimal solution. Fig. 6 displays the Branch-and-Price scheme.

First, the linear relaxation of the path formulation (Master problem) is solved using column generation algorithm. We start solving the linear relaxation of the Restricted Master Problem (obtained from the master problem by considering only a small number of variables). Then, additional variables (columns) are iteratively generated by solving the pricing problem. If no column (with negative reduced cost) is generated, the optimal solution for the linear relaxation is found. Often, the solution of the linear relaxation is not integer. Then, we apply the branching rules (see Section 5.2) to split the domain of the fractional variable into two sub-domains generating two branching nodes. The mechanism is then repeated on each of the new branching nodes.

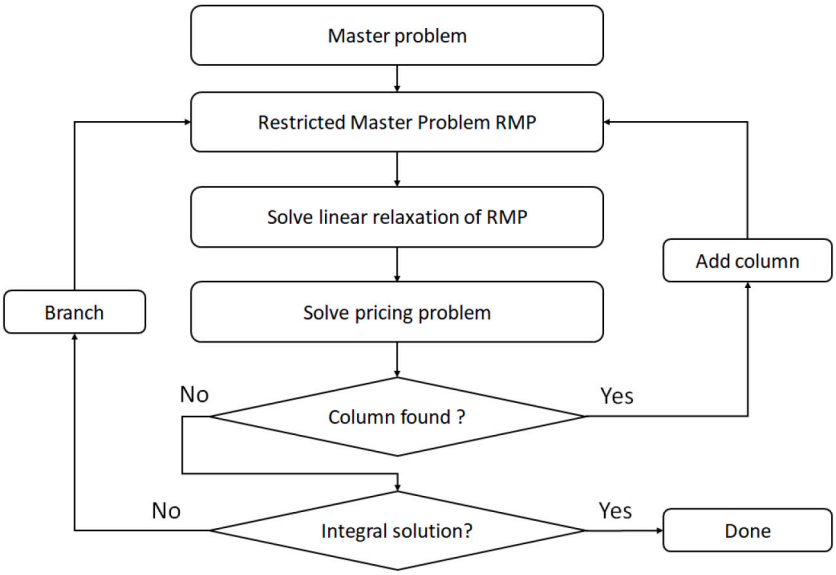

Fig. 6. Scheme of the Branch-and-Price algorithm.

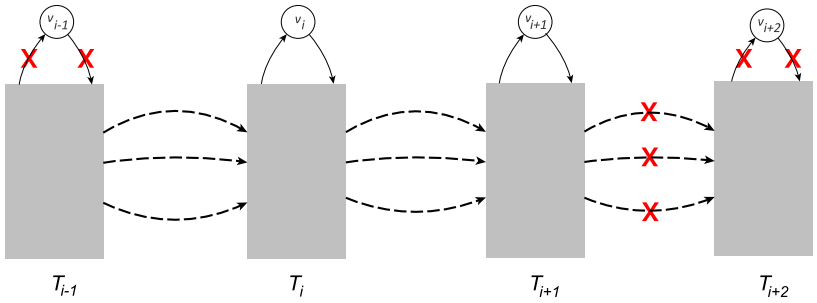

Fig. 7. Illustration of the graph transformation for solving the pricing problem of CFSPTP. All ingress arcs of T_{i+2} and all dummy arcs of v_{i-1} and v_{i+2} are removed.

Note that traditional branching rules on binary variables are not suitable since variables set to 0 are re-generated in the next column generation iterations, and it is difficult to take into account the branching decisions in the pricing problems.

The remaining classical mechanisms of the Branch-and-Bound algorithm are also applied (updating the lower and upper bounds, pruning strategy...etc.). In our implementation, we consider a depth-first search strategy to explore the branching tree.

6. Extension to other variants

In this section, we extend the Branch-and-Price algorithm proposed in this paper for other variants of the CSPTP. In particular, we consider the CFSPTP problem presented in Carrabs et al. (2020), and another variant where each subset of $\mathcal{T}$ must be visited only once.

Constrained forward shortest path tour problem (CFSPTP). To solve this problem, we only modify the graph used for the pricing problem associated with $i \in \{0, \dots, k\}$, by removing all the arcs of $\delta^-(v)$ for each $v \in T_j$ where $j > (i+1)$ (see Fig. 7).

Constrained strict shortest path tour problem (CSSPTP). This problem consists in finding a path p from s to t such that each set of $\mathcal{T}$ is crossed only once in the given order, i.e., $|p \cap T_i| = 1$ for each $i \in \{1, \dots, k\}$ and for two subsets $i < j \in \{0, \dots, (k+1)\}$ the node in $p \cap T_i$ is before the node in $p \cap T_j$ in the path. To solve this problem, we only modify the graph used for the pricing problem associated with $i \in \{1, \dots, k\}$, by removing the arcs of $\delta^-(v)$ for each $v \in T_j$ where $j \in \{0, \dots, (k+1)\} \setminus \{i+1\}$ (see Fig. 8).

These two transformations do not modify the original master problem and thus the branching scheme. All variants can be considered using our framework with similar performance. In particular, we can solve the constrained shortest path problem with node inclusion (i.e., CSPNI), which is a particular case of CSSPTP where each set is a singleton.

7. Numerical results

The Branch-and-Price algorithm described in the previous sections has been implemented in C++, using CPLEX v12.6 (IBM, 2013) as an LP-solver and the LEMON (Dezs et al., 2011) library for the shortest path algorithm. It was tested on a server equipped with an Intel(R) Xeon(R) CPU E5-4627 v2 of 3.30 GHz (32 cores), 504 GB of RAM and running under Linux 64 bits. A maximum of 1 thread has been used and the time limit has been set to 1800 s. Remark that all computational times presented in this section include the construction of graph extension and preprocessing. For each instance, we compute the density as follow: $\frac{100 \times \text{number of links}}{(\text{number of nodes})(\text{number of nodes-1})}$. In this section, we present evaluation results on three types of instances

(1) *IPRAN* instances: 149 instances that are typical from Radio Access Networks (RAN) which are IP (Internet Protocol) networks where the topology has a hierarchical structure (Huin et al., 2019): there is a core layer, to which several aggregation layers are connected, being themselves connected to several access layers. Each layer corresponds to one or more domains, i.e., logical subnets composed by routers and switches, to ease management and ensure scalability. Two types of IPRAN instances are used:

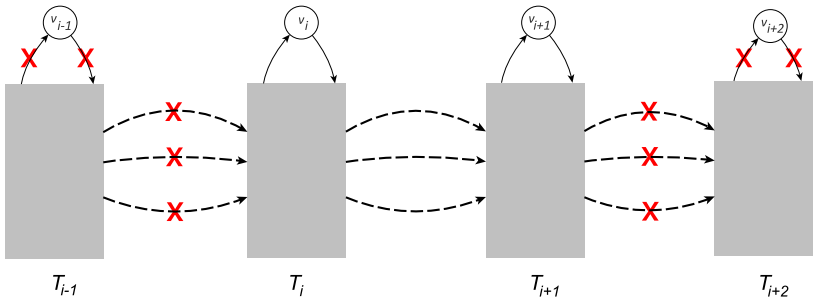

Fig. 8. Illustration of the graph transformation for solving the pricing problem of CSSPTP. All ingress arcs of T_i and T_{i+2} and all dummy arcs of v_{i-1} and v_{i+2} are removed.

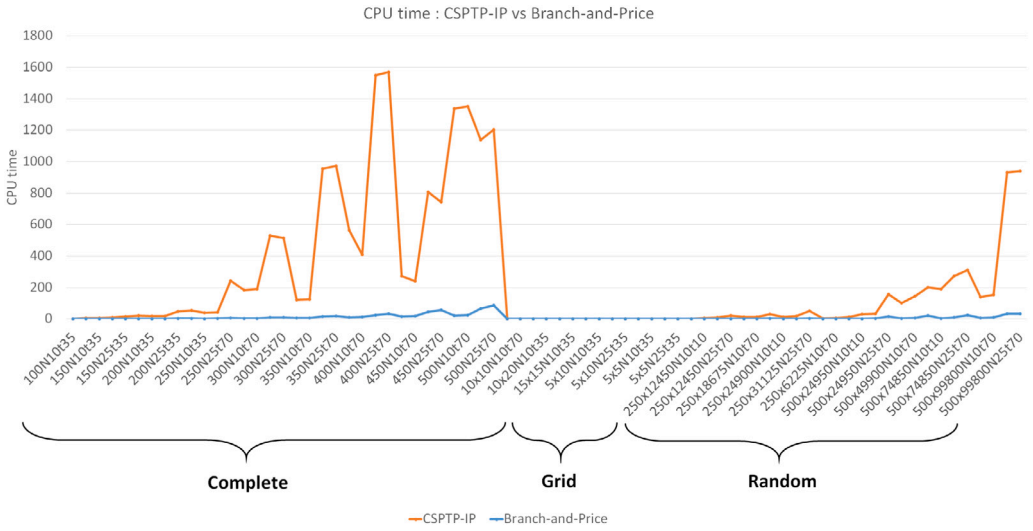

Fig. 9. CPU times comparison (in seconds) between the compact model CSPTP-IP and the Branch-and-Price algorithm on Literature instances (i.e., Complete, Grid, Random). The naming of instances follows: number of vertices "N" (resp. number of vertices x number of arcs) for Complete and Grid (resp. Random), number of inclusion sets "t" and the total number of nodes in inclusion sets.

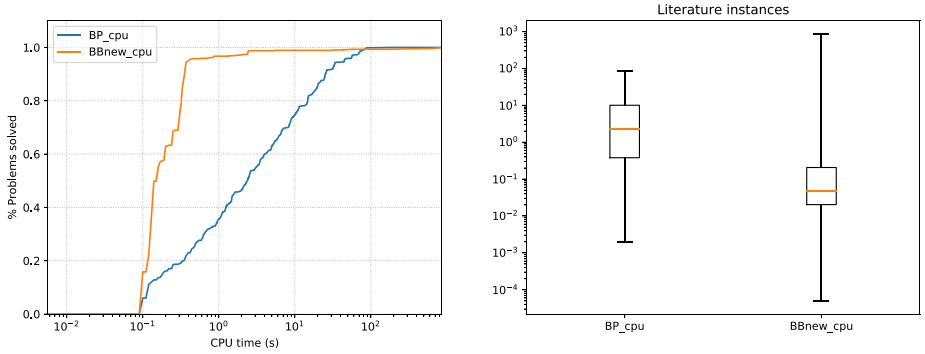

Fig. 10. CPU times comparison (in seconds) on Literature instances between $B\&B^{new}$ and Branch-and-Price (BP) algorithms. All instances have been solved by the two algorithms.

one type with around 1275 nodes and 0.30% of density, and another one with around 5030 nodes and 0.06% of density. The number of inclusion subsets is varied over $2, 4, 6, 8$ and 10 with a maximum size of 1,10 and 20 vertices.

(2) *Random* instances: 240 instances that are randomly generated. For each instance, we start with $n \in \{1000, 2000, 3000\}$ nodes and we add arcs at random between pairs of vertices until the graph is connected and the desired density $d \in \{1\%, 2\%, 5\%, 20\%, 40\%\}$ is reached. Then, a source and a destination are randomly selected. To ensure the feasibility of the instance, a path is computed between the source and the destination, and k disjoints inclusion sets are randomly generated, each one containing at least one node of the path, respect to the order of the nodes in the path. The lengths of arcs on the path are highly increased. The number of inclusion subsets is varied over $1, 5, 10$ and 20 with a maximum size of $1, 5, 10$ and 20.[1]

(3) *Literature* instances: 734 instances that are composed of 3 types of graphs: Complete, Grid and Random graphs, as described in Ferone et al. (2020) by Ferone et al.The number of nodes of the graphs varies between 27 and 500 nodes with densities between 0.98% and 83.43%.

[1] Random instances and the code of our Branch-and-Price (BP) algorithm will be made public. Instances are already available here: https://github.com/MagYou/Constrained-Shortest-path-tour-problem.

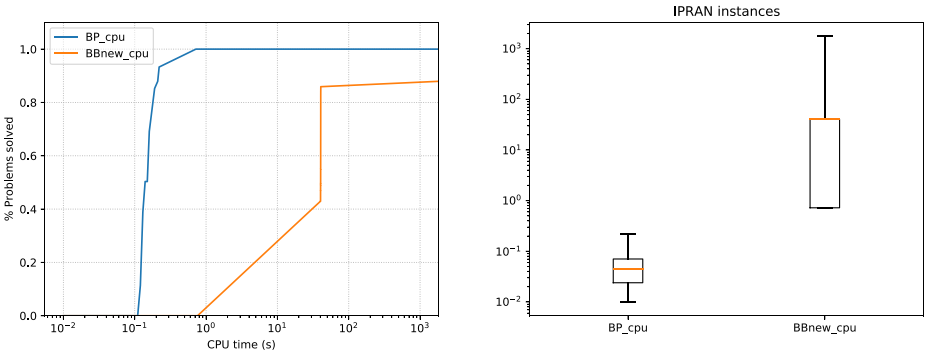

Fig. 11. CPU times comparison (in seconds) on IPRAN instances between $B\&B^{new}$ and Branch-and-Price (BP) algorithms. $B\&B^{new}$ failed to solve 18 instances.

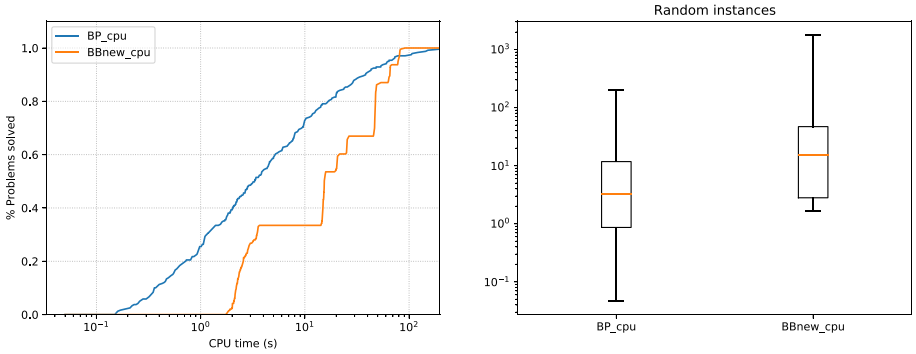

Fig. 12. CPU times comparison (in seconds) on Random instances between $B\&B^{new}$ and Branch-and-Price (BP) algorithms. $B\&B^{new}$ failed to solve 1 instance.

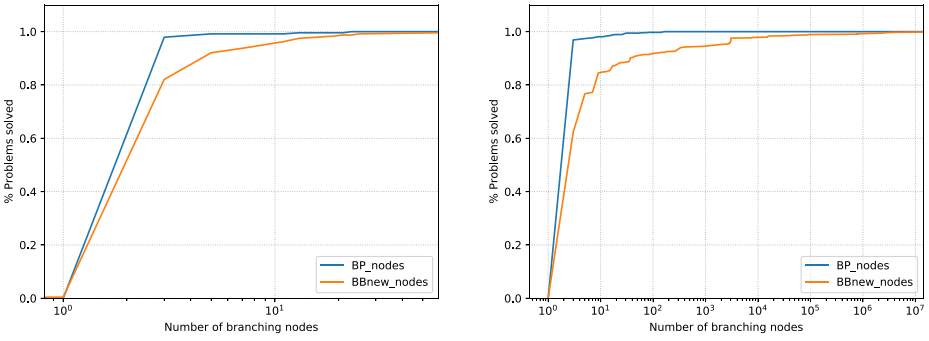

Fig. 13. Number of Branching nodes on Random and Literature instances (instances solved in less than 5000 nodes for Literature) for $B\&B^{new}$ and Branch-and-Price (BP) algorithms.

Fig. 9 shows comparison of CPU times between the compact model CSPTP-IP and the Branch-and-Price algorithm associated the extended model CSPTP-CG, on some Literature instances. It is easy to see that the Branch-and-Price algorithm performs much better than CSPTP-IP. Indeed, CSPTP-CG has less constraints than CSPTP-IP, $(k + |A| + \sum_{i\in\{1,\dots,k\}} |T_i| < k \times |V| + |A| + \sum_{i\in\{1,\dots,k\}} |T_i|)$. Even if the number of variables can be greater in CSPTP-CG than in CSPTP-IP, in reality, the number of generated variables is limited. Note that the difficulty introduced by the interdiction to cross a link twice does not appear in the extended graph. Only some paths associated with consecutive inclusion vertices can cross the same link. This implies that only some consecutive inclusion vertices need lot of paths/variables and the other consecutive inclusion vertices need few paths/variables.

In the following numerical results we only compare the Branch-and-Price algorithm with the $B\&B^{new}$ algorithm presented in Ferone et al. (2020) on the same machine.

Figs. 10–12 display the performance profile and box plots comparing the CPU times of the two algorithms on Literature, IPRAN and Random instances. Box plots summarize several useful information as it displays quartiles and the median. In principle, box plots show the minimum value, first quartile Q_1, median, third quartile Q_3 and the maximum value.

In Fig. 10, we notice that both algorithms solve almost all Literature instances in less than 100 s. Remark that both methods find these instances typically easy. $B\&B^{new}$ is usually a bit faster, but there are a few instances that are quite hard for $B\&B^{new}$.

On IPRAN instances, the Branch-and-Price algorithm solves all the instances to optimality in less than 1 s. The maximum CPU time for the Branch-and-Price algorithm is 0.22 s. $B\&B^{new}$ was unable to solve within the time limit for almost 15% of the instances, and took significantly longer on those that were solved (up to 40 s). This is due to the low density of IPRAN instances. The computational time of our algorithm depends more on the number of links and the size of the tour, whereas the computational time of $B\&B^{new}$ depends also on the number of nodes.

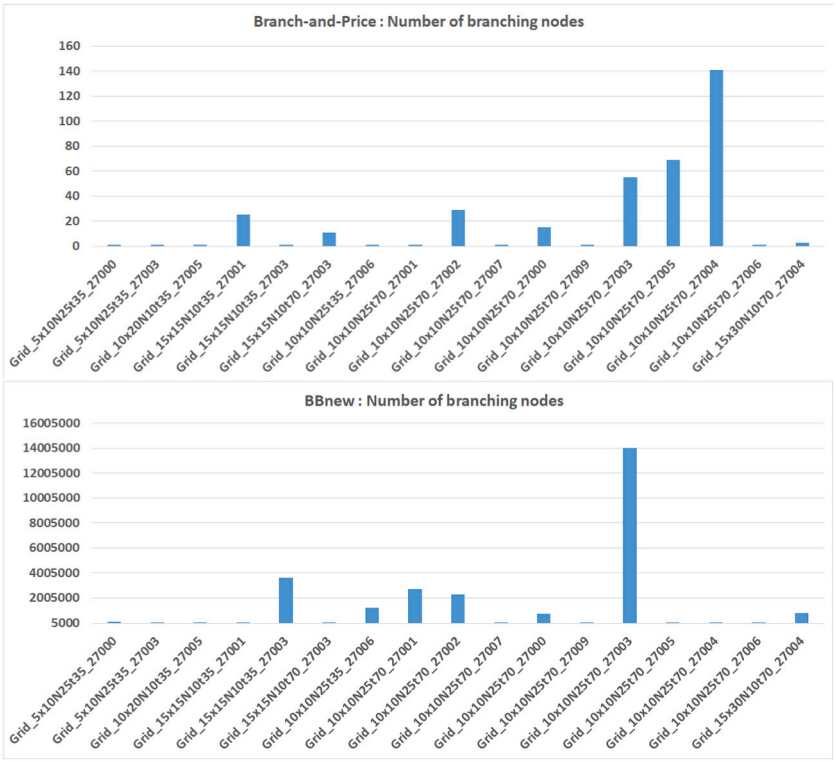

Fig. 14. Number of Branching nodes on Literature instances (instances solved in more than 5000 nodes for Literature) for $B\&B^{new}$ and Branch-and-Price (BP) algorithms (same naming of instances as Fig. 9).

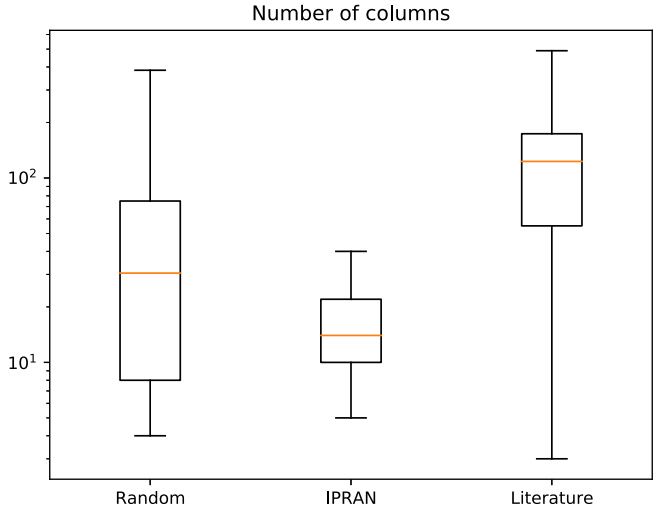

Fig. 15. Number of generated columns by Branch-and-Price algorithm.

On Random instances in Fig. 12, we notice that the Branch-and-Price algorithm performs much better than $B\&B^{new}$ algorithm. Indeed, 85% of the instances have been solved in less than 25 s compared to 50 s for the $B\&B^{new}$ algorithm. We remark that on some instances $B\&B^{new}$ obtains better results. The maximum CPU time for the Branch-and-Price algorithm is 197.80 s.

Figs. 13 and 14 show the numerical results comparing the number of branching nodes for the two algorithms (Branch-and-Price and $B\&B^{new}$). Only Random and Literature instances are considered as all solved IPRAN do not generate more than 1 node in the branching tree, by both algorithms. Moreover, for the sake of clarity, we have separated the plots for Literature instances: those solved in less (resp. more) than 5000 branching nodes are shown in Fig. 13 (resp. 14).

Fig. 13 displays performance profiles. We notice that almost all Literature instances have been solved in the first branching node by the Branch-and-Price algorithm while 90% of these instances are solved in the first branching node by $B\&B^{new}$ algorithm. For Random instances, almost all instances are solved in less than 5 and 30 branching nodes by the Branch-and-Price and $B\&B^{new}$ algorithms, respectively.

Fig. 14 compares the number of Branching nodes of the two algorithms on 17 Literature instances requiring at least 5000 nodes by $B\&B^{new}$ algorithm. We notice that the Branch-and-Price algorithm solves all instances in less than 140 s while $B\&B^{new}$ algorithm reaches millions of branching nodes on 2 instances and several thousands of branching nodes on the remaining ones.

Fig. 15 shows a box plot representing the number of generated columns by the Branch-and-Price algorithm for the three types of instances. On most of Random instances, the algorithm generates less than 80 columns (on 50% of the instances require less than 40 columns), while the Literature instances require 200 columns by most of them. We notice that the IPRAN instances have been solved by very small number of iterations (around 20 columns). This can be explained by the fact that all these instances have been solved in the root node of the branching tree (only one column generation phase by instance).

8. Conclusion

In this paper, we have considered the constrained shortest path tour problem that occurs, for instance, in telecommunication networks for service function chaining. We proved that the problem is NP-hard even when only one vertex need to be included, i.e. only one set of inclusions with one singleton. We proposed a graph transformation to consider a new compact formulation of the problem that helps decomposing it. Based on this formulation, we developed an efficient Branch-and-Price algorithm where several variants of the CSPTP can be considered by

Table 1
Numerical results comparing the Branch-and-Price and $B\&B^{new}$ algorithms on IPRAN instances.

instanceName	nbSet	maxSize	nbNodes	density	BP_value	BP_nodes	BP_gap	BP_cols	BP_cpu	BBnew_value	BBnew_nodes	BBnew_cpu
middle_flexE_4_2_1	2	1	1275	0.15	5092	1	0.00	5	0.01	5092	1	0.72
middle_flexE_1_2_1	2	1	1275	0.15	5089	1	0.00	7	0.01	5089	1	0.72
middle_flexE_2_2_1	2	1	1275	0.15	12703	1	0.00	8	0.01	12703	1	0.72
middle_flexE_3_2_1	2	1	1275	0.16	7631	1	0.00	6	0.01	7631	1	0.72
middle_flexE_5_2_1	2	1	1275	0.16	2546	1	0.00	5	0.01	2546	1	0.72
middle_flexE_4_2_10	2	10	1275	0.15	7631	1	0.00	7	0.01	7631	1	0.72
middle_flexE_2_2_10	2	10	1275	0.16	10165	1	0.00	11	0.01	10165	1	0.72
middle_flexE_1_2_10	2	10	1275	0.16	2547	1	0.00	7	0.01	2547	1	0.72
middle_flexE_3_2_10	2	10	1275	0.16	5087	1	0.00	5	0.01	5087	1	0.72
middle_flexE_5_2_10	2	10	1275	0.16	2544	1	0.00	7	0.01	2544	1	0.72
middle_flexE_1_2_20	2	20	1275	0.15	2546	1	0.00	5	0.01	2546	1	0.72
middle_flexE_4_2_20	2	20	1275	0.16	7631	1	0.00	8	0.01	7631	1	0.72
middle_flexE_3_2_20	2	20	1275	0.16	2545	1	0.00	7	0.01	2545	1	0.72
middle_flexE_2_2_20	2	20	1275	0.16	8	1	0.00	6	0.01	8	1	0.72
middle_flexE_5_2_20	2	20	1275	0.16	5087	1	0.00	6	0.01	5087	1	0.72
middle_flexE_4_4_1	4	1	1277	0.15	2550	1	0.00	9	0.01	2550	1	0.73
middle_flexE_1_4_1	4	1	1277	0.15	10175	1	0.00	13	0.02	10175	1	0.72
middle_flexE_2_4_1	4	1	1277	0.15	10170	1	0.00	11	0.02	10170	1	0.72
middle_flexE_3_4_1	4	1	1277	0.16	10175	1	0.00	10	0.01	10175	1	0.72
middle_flexE_5_4_1	4	1	1277	0.16	12714	1	0.00	9	0.02	12714	1	0.72
middle_flexE_4_4_10	4	10	1277	0.16	5093	1	0.00	13	0.02	5093	1	0.73
middle_flexE_1_4_10	4	10	1277	0.16	5093	1	0.00	10	0.02	5093	1	0.73
middle_flexE_2_4_10	4	10	1277	0.16	11	1	0.00	9	0.02	11	1	0.72
middle_flexE_3_4_10	4	10	1277	0.16	5090	1	0.00	12	0.02	5090	1	0.72
middle_flexE_5_4_10	4	10	1277	0.16	5092	1	0.00	13	0.02	5092	1	0.72
middle_flexE_5_4_20	4	20	1277	0.16	2551	1	0.00	11	0.02	2551	1	0.72
middle_flexE_2_4_20	4	20	1277	0.16	2548	1	0.00	12	0.03	2548	1	0.72
middle_flexE_4_4_20	4	20	1277	0.16	9	1	0.00	9	0.03	9	1	0.72
middle_flexE_3_4_20	4	20	1277	0.16	7632	1	0.00	20	0.04	7632	1	0.72
middle_flexE_4_6_1	6	1	1279	0.15	2557	1	0.00	14	0.02	2557	1	0.72
middle_flexE_1_6_1	6	1	1279	0.15	5099	1	0.00	12	0.02	5099	1	0.72
middle_flexE_2_6_1	6	1	1279	0.15	7638	1	0.00	14	0.02	7638	1	0.73
middle_flexE_3_6_1	6	1	1279	0.16	10180	1	0.00	13	0.02	10180	1	0.72
middle_flexE_5_6_1	6	1	1279	0.16	2558	1	0.00	10	0.02	2558	1	0.72
middle_flexE_1_6_10	6	10	1279	0.16	7637	1	0.00	16	0.02	7637	1	0.73
middle_flexE_4_6_10	6	10	1279	0.16	12717	1	0.00	21	0.02	12717	1	0.72
middle_flexE_5_6_10	6	10	1279	0.16	5097	1	0.00	17	0.02	5097	1	0.72
middle_flexE_3_6_10	6	10	1279	0.16	5095	1	0.00	14	0.02	5095	1	0.72
middle_flexE_2_6_10	6	10	1279	0.16	10177	1	0.00	19	0.03	10177	1	0.72
middle_flexE_4_6_20	6	20	1279	0.16	10176	1	0.00	20	0.03	10176	1	0.73
middle_flexE_1_6_20	6	20	1279	0.16	7637	1	0.00	22	0.04	−1	1	1800.00
middle_flexE_2_6_20	6	20	1279	0.16	10168	1	0.00	18	0.04	10168	1	0.72
middle_flexE_5_6_20	6	20	1279	0.16	10180	1	0.00	17	0.04	10180	1	0.72
middle_flexE_3_6_20	6	20	1279	0.17	15259	1	0.00	36	0.08	15259	1	0.72
middle_flexE_4_8_1	8	1	1281	0.15	15262	1	0.00	18	0.02	15262	1	0.72
middle_flexE_1_8_1	8	1	1281	0.15	12721	1	0.00	16	0.02	12721	1	0.72
middle_flexE_2_8_1	8	1	1281	0.15	15259	1	0.00	18	0.02	15259	1	0.72
middle_flexE_3_8_1	8	1	1281	0.16	2566	1	0.00	13	0.02	2566	1	0.72
middle_flexE_5_8_1	8	1	1281	0.16	5102	1	0.00	13	0.02	5102	1	0.72
middle_flexE_1_8_10	8	10	1281	0.16	15265	1	0.00	22	0.03	15265	1	0.72
middle_flexE_3_8_10	8	10	1281	0.16	17804	1	0.00	28	0.04	17804	1	0.72
middle_flexE_4_8_10	8	10	1281	0.16	10182	1	0.00	22	0.04	10182	1	0.72
middle_flexE_2_8_10	8	10	1281	0.16	17795	1	0.00	29	0.05	17795	1	0.72
middle_flexE_5_8_10	8	10	1281	0.16	7643	1	0.00	20	0.04	7643	1	0.72
middle_flexE_4_8_20	8	20	1281	0.16	7640	1	0.00	23	0.05	−1	1	1800.00
middle_flexE_3_8_20	8	20	1281	0.16	10181	1	0.00	19	0.05	−1	1	1800.00
middle_flexE_2_8_20	8	20	1281	0.16	15254	1	0.00	25	0.06	−1	1	1800.00
middle_flexE_1_8_20	8	20	1281	0.16	10181	1	0.00	26	0.07	10181	1	0.74
middle_flexE_5_8_20	8	20	1281	0.17	12722	1	0.00	29	0.08	12722	1	0.76
middle_flexE_4_10_1	10	1	1283	0.15	15270	1	0.00	24	0.03	15270	1	0.72
middle_flexE_1_10_1	10	1	1283	0.15	20348	1	0.00	19	0.03	20348	1	0.72
middle_flexE_2_10_1	10	1	1283	0.16	25415	1	0.00	23	0.03	25415	1	0.72
middle_flexE_3_10_1	10	1	1283	0.16	5106	1	0.00	17	0.03	5106	1	0.72
middle_flexE_5_10_1	10	1	1283	0.16	15264	1	0.00	21	0.03	−1	1	1800.00
middle_flexE_2_10_10	10	10	1283	0.16	17801	1	0.00	24	0.04	17801	1	0.72
middle_flexE_4_10_10	10	10	1283	0.16	10185	1	0.00	27	0.05	10185	1	0.72
middle_flexE_1_10_10	10	10	1283	0.16	10186	1	0.00	40	0.07	−1	1	1800.00
middle_flexE_3_10_10	10	10	1283	0.16	15271	1	0.00	30	0.06	−1	1	1800.00

(*continued on next page*)

only applying graph filtering. The branching scheme proposed allows keeping the shortest path algorithm to solve the pricing problem. Our computational results has shown the efficiency of the Branch-and-Price algorithm compared to state of art. On a diverse set of instances, we show that our algorithm significantly improves the maximum solution time while the ranking of algorithms for the average varies over instances.

Table 1 (*continued*).

instanceName	nbSet	maxSize	nbNodes	density	BP_value	BP_nodes	BP_gap	BP_cols	BP_cpu	BBnew_value	BBnew_nodes	BBnew_cpu
middle_flexE_5_10_10	10	10	1283	0.16	15 265	1	0.00	25	0.05	15 265	1	0.72
middle_flexE_4_10_20	10	20	1283	0.16	10 184	1	0.00	32	0.11	10 184	1	0.72
middle_flexE_2_10_20	10	20	1283	0.17	20 339	1	0.00	39	0.13	−1	1	1800.00
middle_flexE_1_10_20	10	20	1283	0.17	7646	1	0.00	30	0.11	7646	1	0.72
middle_flexE_5_10_20	10	20	1283	0.17	5107	1	0.00	30	0.11	−1	1	1800.00
middle_flexE_3_10_20	10	20	1283	0.17	20 349	1	0.00	34	0.15	−1	1	1800.00
large_2_2_1	2	1	5025	0.03	40 169	1	0.00	8	0.04	40 169	1	40.38
large_3_2_1	2	1	5025	0.03	20 086	1	0.00	5	0.03	20 086	1	40.33
large_4_2_1	2	1	5025	0.03	20 088	1	0.00	5	0.03	20 088	1	40.30
large_5_2_1	2	1	5025	0.03	10 047	1	0.00	5	0.03	10 046	1	40.29
large_1_2_1	2	1	5025	0.03	8	1	0.00	5	0.03	8	1	40.17
large_3_2_10	2	10	5025	0.03	20 087	1	0.00	8	0.04	20 087	1	40.48
large_2_2_10	2	10	5025	0.03	10 047	1	0.00	5	0.03	10 047	1	40.20
large_4_2_10	2	10	5025	0.03	20 090	1	0.00	8	0.04	20 090	1	40.34
large_5_2_10	2	10	5025	0.03	7	1	0.00	5	0.03	7	1	40.18
large_1_2_10	2	10	5025	0.03	10 048	1	0.00	8	0.04	10 048	1	40.48
large_2_2_20	2	20	5025	0.03	10 045	1	0.00	5	0.03	10 044	1	40.43
large_4_2_20	2	20	5025	0.03	10 045	1	0.00	5	0.03	10 045	1	40.33
large_3_2_20	2	20	5025	0.03	10 045	1	0.00	6	0.04	10 045	1	40.40
large_5_2_20	2	20	5025	0.03	10 043	1	0.00	8	0.05	10 043	1	40.39
large_1_2_20	2	20	5025	0.03	10 045	1	0.00	6	0.04	10 045	1	40.33
large_2_4_1	4	1	5027	0.03	10 054	1	0.00	9	0.04	10 054	1	40.51
large_3_4_1	4	1	5027	0.03	10 051	1	0.00	9	0.04	10 051	1	40.28
large_4_4_1	4	1	5027	0.03	30 135	1	0.00	9	0.04	30 135	1	40.45
large_5_4_1	4	1	5027	0.03	30 125	1	0.00	11	0.05	30 125	1	40.38
large_1_4_1	4	1	5027	0.03	20 091	1	0.00	11	0.05	20 091	1	40.39
large_3_4_10	4	10	5027	0.03	20 090	1	0.00	10	0.05	20 089	1	40.37
large_2_4_10	4	10	5027	0.03	20 097	1	0.00	10	0.05	20 096	1	40.37
large_4_4_10	4	10	5027	0.03	40 176	1	0.00	14	0.05	40 176	1	40.37
large_5_4_10	4	10	5027	0.03	20 090	1	0.00	13	0.05	20 090	1	40.32
large_1_4_10	4	10	5027	0.03	20 093	1	0.00	12	0.05	20 093	1	40.34
large_2_4_20	4	20	5027	0.03	30 130	1	0.00	12	0.05	30 130	1	40.42
large_3_4_20	4	20	5027	0.03	50 214	1	0.00	13	0.06	50 214	1	40.38
large_4_4_20	4	20	5027	0.03	20 092	1	0.00	10	0.06	20 092	1	40.21
large_1_4_20	4	20	5027	0.03	30 133	1	0.00	13	0.06	30 133	1	40.34
large_5_4_20	4	20	5027	0.03	50 203	1	0.00	14	0.07	50 203	1	40.30
large_2_6_1	6	1	5029	0.03	10 059	1	0.00	11	0.06	10 059	1	40.40
large_3_6_1	6	1	5029	0.03	20 096	1	0.00	13	0.05	20 096	1	40.39
large_4_6_1	6	1	5029	0.03	40 177	1	0.00	14	0.06	40 176	1	40.36
large_5_6_1	6	1	5029	0.03	20 094	1	0.00	10	0.05	20 094	1	40.19
large_1_6_1	6	1	5029	0.03	21	1	0.00	12	0.05	21	1	40.36
large_3_6_10	6	10	5029	0.03	20	1	0.00	17	0.07	20	1	40.36
large_2_6_10	6	10	5029	0.03	30 142	1	0.00	19	0.07	−1	1	1800.00
large_4_6_10	6	10	5029	0.03	50 219	1	0.00	16	0.06	50 219	1	40.29
large_5_6_10	6	10	5029	0.03	20 089	1	0.00	11	0.06	20 089	1	40.33
large_1_6_10	6	10	5029	0.03	40 177	1	0.00	19	0.07	40 177	1	40.30
large_3_6_20	6	20	5029	0.03	10 059	1	0.00	18	0.08	10 059	1	40.33
large_2_6_20	6	20	5029	0.03	17	1	0.00	14	0.07	17	1	40.37
large_4_6_20	6	20	5029	0.03	30 141	1	0.00	18	0.08	30 141	1	40.16
large_1_6_20	6	20	5029	0.03	50 220	1	0.00	20	0.09	−1	1	1800.00
large_5_6_20	6	20	5029	0.03	30 133	1	0.00	20	0.10	30 133	1	40.36
large_2_8_1	8	1	5031	0.03	80 339	1	0.00	21	0.07	80 339	1	40.29
large_3_8_1	8	1	5031	0.03	30 144	1	0.00	12	0.06	30 143	1	40.53
large_4_8_1	8	1	5031	0.03	50 221	1	0.00	17	0.07	50 221	1	40.23
large_5_8_1	8	1	5031	0.03	40 178	1	0.00	14	0.06	40 178	1	40.35
large_1_8_1	8	1	5031	0.03	10 063	1	0.00	21	0.07	10 063	1	40.32
large_2_8_10	8	10	5031	0.03	60 254	1	0.00	26	0.10	60 254	1	40.25
large_4_8_10	8	10	5031	0.03	30 144	1	0.00	21	0.09	−1	1	1800.00
large_3_8_10	8	10	5031	0.03	40 181	1	0.00	22	0.09	40 181	1	40.60
large_5_8_10	8	10	5031	0.03	40 173	1	0.00	18	0.08	40 173	1	40.41
large_1_8_10	8	10	5031	0.03	70 302	1	0.00	22	0.08	70 302	1	40.39
large_2_8_20	8	20	5031	0.03	40 179	1	0.00	23	0.10	40 179	1	40.34
large_4_8_20	8	20	5031	0.03	30 142	1	0.00	22	0.11	−1	1	1800.00
large_3_8_20	8	20	5031	0.03	40 182	1	0.00	29	0.14	−1	1	1800.00
large_1_8_20	8	20	5031	0.03	30 145	1	0.00	21	0.10	30 145	1	40.17
large_5_8_20	8	20	5031	0.03	50 211	1	0.00	29	0.14	50 211	1	40.18
large_2_10_1	10	1	5033	0.03	30 149	1	0.00	18	0.07	30 149	1	40.33
large_3_10_1	10	1	5033	0.03	60 267	1	0.00	23	0.08	60 267	1	40.35
large_4_10_1	10	1	5033	0.03	50 225	1	0.00	21	0.08	−1	1	1800.00
large_5_10_1	10	1	5033	0.03	30 142	1	0.00	16	0.07	30 142	1	40.39

(*continued on next page*)

An interesting perspective could be the analysis of valid inequalities, theoretically with facet defining proofs and computationally with a Branch-and-Cut-and-Price algorithm to strengthen the model and reduce the computational time.

Table 1 (*continued*).

instanceName	nbSet	maxSize	nbNodes	density	BP_value	BP_nodes	BP_gap	BP_cols	BP_cpu	BBnew_value	BBnew_nodes	BBnew_cpu
large_1_10_1	10	1	5033	0.03	60 270	1	0.00	19	0.08	60 270	1	40.40
large_2_10_10	10	10	5033	0.03	60 269	1	0.00	29	0.11	60 269	1	40.34
large_4_10_10	10	10	5033	0.03	60 267	1	0.00	27	0.12	60 267	1	40.35
large_3_10_10	10	10	5033	0.03	60 266	1	0.00	28	0.12	60 265	1	40.41
large_5_10_10	10	10	5033	0.03	50 217	1	0.00	35	0.13	50 217	1	40.34
large_1_10_10	10	10	5033	0.03	50 227	1	0.00	27	0.12	50 227	1	40.37
large_2_10_20	10	20	5033	0.03	80 344	1	0.00	31	0.16	−1	1	1800.00
large_5_10_20	10	20	5033	0.03	60 252	1	0.00	34	0.16	60 252	1	40.39
large_4_10_20	10	20	5033	0.03	40 187	1	0.00	39	0.22	40 187	1	40.28
large_3_10_20	10	20	5033	0.03	40 187	1	0.00	31	0.19	40 187	1	40.41
large_1_10_20	10	20	5033	0.03	80 344	1	0.00	34	0.21	−1	1	1800.00

Table 2
Numerical results comparing the Branch-and-Price and $B\&B^{new}$ algorithms on Random instances.

instanceName	nbSet	maxSize	nbNodes	density	BP_value	BP_nodes	BP_gap	BP_cols	BP_cpu	BBnew_value	BBnew_nodes	BBnew_cpu
r_1_1_1000_2	1	1	1003	1.09	89	1	0.00	4	0.05	89	1	2.47
r_1_1_1000_4	1	1	1003	2.09	97	1	0.00	4	0.09	97	1	2.41
r_1_1_1000_10	1	1	1003	5.07	27	1	0.00	4	0.21	27	1	2.70
r_1_1_1000_40	1	1	1003	19.98	12	1	0.00	4	0.92	12	1	2.80
r_1_1_1000_80	1	1	1003	39.86	11	1	0.00	4	1.66	11	1	3.41
r_1_5_1000_2	1	5	1003	1.10	142	1	0.00	6	0.06	142	1	2.01
r_1_5_1000_4	1	5	1003	2.09	57	1	0.00	6	0.11	57	1	2.02
r_1_5_1000_10	1	5	1003	5.07	30	1	0.00	4	0.23	30	1	2.04
r_1_5_1000_40	1	5	1003	19.98	11	1	0.00	6	0.93	11	1	2.04
r_1_5_1000_80	1	5	1003	39.86	8	1	0.00	6	2.05	8	1	3.25
r_1_10_1000_2	1	10	1003	1.10	168	1	0.00	8	0.06	168	3	2.40
r_1_10_1000_4	1	10	1003	2.09	55	1	0.00	8	0.12	55	1	2.73
r_1_10_1000_10	1	10	1003	5.07	38	1	0.00	6	0.29	38	1	2.28
r_1_10_1000_40	1	10	1003	19.98	11	1	0.00	8	0.99	11	1	2.44
r_1_10_1000_80	1	10	1003	39.86	8	1	0.00	4	1.96	8	1	3.36
r_1_20_1000_2	1	20	1003	1.10	116	1	0.00	8	0.07	116	1	2.10
r_1_20_1000_4	1	20	1003	2.09	49	1	0.00	10	0.15	49	1	1.98
r_1_20_1000_10	1	20	1003	5.07	27	1	0.00	8	0.28	27	1	2.04
r_1_20_1000_40	1	20	1003	19.98	13	1	0.00	12	1.48	13	1	2.22
r_1_20_1000_80	1	20	1003	39.86	8	1	0.00	13	3.30	8	1	3.08
r_5_1_1000_2	5	1	1007	1.09	430	1	0.00	8	0.10	430	1	1.68
r_5_1_1000_4	5	1	1007	2.07	174	1	0.00	8	0.17	174	1	1.78
r_5_1_1000_10	5	1	1007	5.03	122	1	0.00	8	0.39	122	1	2.05
r_5_1_1000_40	5	1	1007	19.82	34	1	0.00	8	1.70	34	1	2.27
r_5_1_1000_80	5	1	1007	39.55	31	1	0.00	8	3.82	31	1	3.15
r_5_5_1000_2	5	5	1007	1.09	379	1	0.00	26	0.16	379	1	2.48
r_5_5_1000_4	5	5	1007	2.08	166	1	0.00	32	0.26	166	3	2.62
r_5_5_1000_10	5	5	1007	5.03	90	1	0.00	25	0.59	90	1	2.71
r_5_5_1000_40	5	5	1007	19.83	28	1	0.00	21	2.47	28	1	2.83
r_5_5_1000_80	5	5	1007	39.55	21	1	0.00	16	4.33	21	1	3.47
r_5_10_1000_2	5	10	1007	1.09	316	21	2.27	89	0.63	316	13	2.25
r_5_10_1000_4	5	10	1007	2.08	129	1	0.00	32	0.32	129	3	2.12
r_5_10_1000_10	5	10	1007	5.04	75	1	0.00	36	0.80	75	1	1.91
r_5_10_1000_40	5	10	1007	19.83	23	1	0.00	27	2.66	23	1	2.24
r_5_10_1000_80	5	10	1007	39.55	18	1	0.00	32	6.16	18	1	3.00
r_5_20_1000_2	5	20	1007	1.10	173	1	0.00	32	0.17	173	1	2.00
r_5_20_1000_4	5	20	1007	2.09	92	1	0.00	32	0.30	92	1	2.05
r_5_20_1000_10	5	20	1007	5.05	66	1	0.00	72	0.98	66	1	2.19
r_5_20_1000_40	5	20	1007	19.84	19	1	0.00	35	2.79	19	1	2.32
r_5_20_1000_80	5	20	1007	39.56	17	1	0.00	49	7.59	17	1	3.32
r_10_1_1000_2	10	1	1012	1.08	887	1	0.00	15	0.13	887	3	1.81
r_10_1_1000_4	10	1	1012	2.05	422	1	0.00	13	0.22	422	1	2.10
r_10_1_1000_10	10	1	1012	4.98	196	1	0.00	13	0.52	196	1	2.17
r_10_1_1000_40	10	1	1012	19.63	74	1	0.00	15	2.71	74	3	2.48
r_10_1_1000_80	10	1	1012	39.16	53	1	0.00	13	4.62	53	1	3.38
r_10_5_1000_2	10	5	1012	1.08	589	1	0.00	59	0.24	589	7	1.92
r_10_5_1000_4	10	5	1012	2.06	277	1	0.00	55	0.37	277	13	2.06
r_10_5_1000_10	10	5	1012	4.99	129	1	0.00	43	0.84	129	1	2.16
r_10_5_1000_40	10	5	1012	19.64	55	1	0.00	58	3.75	55	3	2.80
r_10_5_1000_80	10	5	1012	39.16	29	1	0.00	32	7.22	29	1	3.41
r_10_10_1000_2	10	10	1012	1.09	461	1	0.00	66	0.25	461	3	1.71
r_10_10_1000_4	10	10	1012	2.07	259	1	0.00	105	0.54	259	1	2.09
r_10_10_1000_10	10	10	1012	5.00	121	1	0.00	80	1.17	121	1	2.53
r_10_10_1000_40	10	10	1012	19.64	45	1	0.00	75	4.45	45	1	2.41
r_10_10_1000_80	10	10	1012	39.17	30	1	0.00	58	7.89	30	1	3.43
r_10_20_1000_2	10	20	1012	1.11	286	1	0.00	101	0.52	286	1	1.92
r_10_20_1000_4	10	20	1012	2.08	205	1	0.00	116	1.01	205	3	1.72
r_10_20_1000_10	10	20	1012	5.01	96	1	0.00	138	2.08	96	1	1.97
r_10_20_1000_40	10	20	1012	19.66	37	1	0.00	68	4.99	37	1	2.80

(*continued on next page*)

Table 2 (*continued*).

instanceName	nbSet	maxSize	nbNodes	density	BP_value	BP_nodes	BP_gap	BP_cols	BP_cpu	BBnew_value	BBnew_nodes	BBnew_cpu
r_10_20_1000_80	10	20	1012	39.19	24	1	0.00	118	12.43	24	1	3.40
r_20_1_1000_2	20	1	1022	1.06	1547	1	0.00	25	0.26	1547	3	2.17
r_20_1_1000_4	20	1	1022	2.02	800	1	0.00	35	0.55	800	23	1.91
r_20_1_1000_10	20	1	1022	4.89	368	1	0.00	25	1.12	368	5	2.20
r_20_1_1000_40	20	1	1022	19.25	136	1	0.00	23	4.26	136	1	2.36
r_20_1_1000_80	20	1	1022	38.40	98	1	0.00	23	8.64	98	1	3.45
r_20_5_1000_2	20	5	1022	1.07	926	1	0.00	101	0.49	926	25	2.12
r_20_5_1000_4	20	5	1022	2.03	568	1	0.00	98	0.86	568	1	2.17
r_20_5_1000_10	20	5	1022	4.90	237	1	0.00	85	1.66	237	7	2.86
r_20_5_1000_40	20	5	1022	19.26	97	1	0.00	76	6.88	97	1	2.58
r_20_5_1000_80	20	5	1022	38.41	65	1	0.00	57	13.19	65	1	3.34
r_20_10_1000_2	20	10	1022	1.09	760	1	0.00	107	0.72	760	7	2.07
r_20_10_1000_4	20	10	1022	2.04	483	1	0.00	194	1.17	483	59	2.22
r_20_10_1000_10	20	10	1022	4.92	194	1	0.00	100	1.74	194	1	2.14
r_20_10_1000_40	20	10	1022	19.28	83	1	0.00	105	7.74	83	1	2.32
r_20_10_1000_80	20	10	1022	38.42	56	1	0.00	116	18.17	56	1	3.33
r_20_20_1000_2	20	20	1022	1.11	634	3	0.08	381	2.92	634	19	1.89
r_20_20_1000_4	20	20	1022	2.07	336	1	0.00	177	2.60	336	1	2.44
r_20_20_1000_10	20	20	1022	4.94	169	1	0.00	169	4.37	169	1	2.64
r_20_20_1000_40	20	20	1022	19.30	61	1	0.00	145	11.86	61	1	2.75
r_20_20_1000_80	20	20	1022	38.45	46	1	0.00	129	19.74	46	1	3.44
r_1_1_2000_2	1	1	2003	1.05	111	1	0.00	4	0.16	111	1	15.09
r_1_1_2000_4	1	1	2003	2.04	51	1	0.00	4	0.36	51	1	15.23
r_1_1_2000_10	1	1	2003	5.04	29	1	0.00	4	0.86	29	1	15.24
r_1_1_2000_40	1	1	2003	19.99	10	1	0.00	4	3.67	10	1	19.95
r_1_1_2000_80	1	1	2003	39.93	7	1	0.00	4	8.06	7	1	25.47
r_1_5_2000_2	1	5	2003	1.05	90	1	0.00	8	0.23	90	1	15.08
r_1_5_2000_4	1	5	2003	2.04	39	1	0.00	6	0.40	39	1	14.82
r_1_5_2000_10	1	5	2003	5.04	24	1	0.00	6	1.06	24	1	14.77
r_1_5_2000_40	1	5	2003	19.99	9	1	0.00	9	5.47	9	1	20.09
r_1_5_2000_80	1	5	2003	39.93	7	1	0.00	7	9.53	7	1	25.08
r_1_10_2000_2	1	10	2003	1.05	75	1	0.00	7	0.24	75	1	14.70
r_1_10_2000_4	1	10	2003	2.04	33	1	0.00	4	0.37	33	1	15.27
r_1_10_2000_10	1	10	2003	5.04	14	1	0.00	6	1.00	14	1	15.19
r_1_10_2000_40	1	10	2003	19.99	9	1	0.00	8	4.94	9	1	20.11
r_1_10_2000_80	1	10	2003	39.93	6	1	0.00	8	9.96	6	1	25.36
r_1_20_2000_2	1	20	2003	1.05	71	1	0.00	10	0.26	71	1	15.08
r_1_20_2000_4	1	20	2003	2.04	37	1	0.00	8	0.46	37	1	14.83
r_1_20_2000_10	1	20	2003	5.04	16	1	0.00	6	1.00	16	1	15.37
r_1_20_2000_40	1	20	2003	19.99	8	1	0.00	7	4.57	8	1	20.08
r_1_20_2000_80	1	20	2003	39.93	6	1	0.00	8	9.79	6	1	25.51
r_5_1_2000_2	5	1	2007	1.04	267	1	0.00	8	0.35	267	1	14.74
r_5_1_2000_4	5	1	2007	2.04	174	1	0.00	10	0.83	174	3	14.81
r_5_1_2000_10	5	1	2007	5.02	78	1	0.00	8	1.91	78	1	14.68
r_5_1_2000_40	5	1	2007	19.91	31	1	0.00	8	7.81	31	1	20.31
r_5_1_2000_80	5	1	2007	39.77	23	1	0.00	8	14.11	23	1	25.47
r_5_5_2000_2	5	5	2007	1.04	159	1	0.00	18	0.43	159	1	14.68
r_5_5_2000_4	5	5	2007	2.04	84	1	0.00	21	0.98	84	1	14.83
r_5_5_2000_10	5	5	2007	5.02	52	1	0.00	13	2.16	52	1	14.55
r_5_5_2000_40	5	5	2007	19.91	24	1	0.00	25	9.81	24	1	19.26
r_5_5_2000_80	5	5	2007	39.77	17	1	0.00	18	20.07	17	1	24.54
r_5_10_2000_2	5	10	2007	1.05	142	1	0.00	30	0.57	142	1	15.24
r_5_10_2000_4	5	10	2007	2.04	69	1	0.00	12	0.72	69	1	15.35
r_5_10_2000_10	5	10	2007	5.02	44	1	0.00	30	3.19	44	1	15.35
r_5_10_2000_40	5	10	2007	19.91	20	1	0.00	31	12.76	20	1	20.55
r_5_10_2000_80	5	10	2007	39.77	16	1	0.00	32	26.52	16	1	25.01
r_5_20_2000_2	5	20	2007	1.05	129	1	0.00	43	0.73	129	3	14.63
r_5_20_2000_4	5	20	2007	2.04	84	1	0.00	71	2.00	84	1	14.54
r_5_20_2000_10	5	20	2007	5.02	40	1	0.00	64	3.76	40	1	15.27
r_5_20_2000_40	5	20	2007	19.91	16	1	0.00	34	11.71	16	1	20.35
r_5_20_2000_80	5	20	2007	39.78	14	1	0.00	60	28.83	14	1	25.30
r_10_1_2000_2	10	1	2012	1.04	464	1	0.00	15	0.47	464	3	14.82
r_10_1_2000_4	10	1	2012	2.03	248	1	0.00	15	0.98	248	5	14.91
r_10_1_2000_10	10	1	2012	4.99	129	1	0.00	13	2.35	129	1	15.42
r_10_1_2000_40	10	1	2012	19.81	52	1	0.00	13	11.52	52	1	20.32
r_10_1_2000_80	10	1	2012	39.57	43	1	0.00	13	23.57	43	1	25.13
r_10_5_2000_2	10	5	2012	1.04	331	1	0.00	38	0.82	331	3	14.73
r_10_5_2000_4	10	5	2012	2.03	211	1	0.00	54	1.81	211	1	15.09
r_10_5_2000_10	10	5	2012	4.99	93	1	0.00	35	3.51	93	3	15.07
r_10_5_2000_40	10	5	2012	19.81	39	1	0.00	38	14.24	39	1	20.28
r_10_5_2000_80	10	5	2012	39.58	30	1	0.00	29	29.54	30	1	25.36
r_10_10_2000_2	10	10	2012	1.04	292	1	0.00	81	1.10	292	1	14.18
r_10_10_2000_4	10	10	2012	2.03	168	1	0.00	74	1.85	168	1	15.58

(*continued on next page*)

Table 2 (*continued*).

instanceName	nbSet	maxSize	nbNodes	density	BP_value	BP_nodes	BP_gap	BP_cols	BP_cpu	BBnew_value	BBnew_nodes	BBnew_cpu
r_10_10_2000_10	10	10	2012	4.99	74	1	0.00	47	4.05	74	1	15.31
r_10_10_2000_40	10	10	2012	19.82	36	1	0.00	36	13.56	36	1	20.55
r_10_10_2000_80	10	10	2012	39.58	28	1	0.00	60	38.38	28	1	25.39
r_10_20_2000_2	10	20	2012	1.05	217	1	0.00	95	1.39	217	1	15.18
r_10_20_2000_4	10	20	2012	2.03	132	1	0.00	107	2.58	132	1	15.70
r_10_20_2000_10	10	20	2012	5.00	64	1	0.00	107	5.98	64	1	15.68
r_10_20_2000_40	10	20	2012	19.82	29	1	0.00	79	21.58	29	1	20.29
r_10_20_2000_80	10	20	2012	39.58	25	1	0.00	77	43.22	25	1	25.16
r_20_1_2000_2	20	1	2022	1.03	924	1	0.00	31	1.18	924	7	15.25
r_20_1_2000_4	20	1	2022	2.01	489	1	0.00	23	1.74	489	3	14.45
r_20_1_2000_10	20	1	2022	4.94	252	1	0.00	23	5.00	252	1	14.22
r_20_1_2000_40	20	1	2022	19.62	98	1	0.00	23	19.82	98	1	20.27
r_20_1_2000_80	20	1	2022	39.18	78	1	0.00	23	39.62	78	1	25.13
r_20_5_2000_2	20	5	2022	1.03	600	1	0.00	70	1.55	600	7	14.86
r_20_5_2000_4	20	5	2022	2.01	342	1	0.00	79	3.06	342	5	14.68
r_20_5_2000_10	20	5	2022	4.95	165	1	0.00	84	7.63	165	3	15.16
r_20_5_2000_40	20	5	2022	19.62	77	1	0.00	82	31.89	77	1	20.30
r_20_5_2000_80	20	5	2022	39.19	55	1	0.00	92	64.01	55	1	25.09
r_20_10_2000_2	20	10	2022	1.04	526	1	0.00	153	2.57	526	7	15.24
r_20_10_2000_4	20	10	2022	2.02	299	3	0.17	213	6.01	299	3	15.01
r_20_10_2000_10	20	10	2022	4.95	144	1	0.00	114	7.95	144	1	14.60
r_20_10_2000_40	20	10	2022	19.62	66	1	0.00	101	36.22	66	1	19.67
r_20_10_2000_80	20	10	2022	39.19	51	1	0.00	115	60.59	51	1	25.29
r_20_20_2000_2	20	20	2022	1.04	442	1	0.00	232	5.23	442	1	14.45
r_20_20_2000_4	20	20	2022	2.02	236	1	0.00	245	9.25	236	1	15.02
r_20_20_2000_10	20	20	2022	4.96	126	1	0.00	267	16.68	126	1	14.82
r_20_20_2000_40	20	20	2022	19.63	58	1	0.00	233	60.90	58	1	20.17
r_20_20_2000_80	20	20	2022	39.20	46	1	0.00	203	106.70	46	1	25.23
r_1_1_3000_2	1	1	3003	1.03	48	1	0.00	4	0.52	48	1	47.75
r_1_1_3000_4	1	1	3003	2.03	34	1	0.00	4	0.84	34	1	47.46
r_1_1_3000_10	1	1	3003	5.02	17	1	0.00	4	2.13	17	1	47.90
r_1_1_3000_40	1	1	3003	19.99	7	1	0.00	4	8.50	7	1	65.31
r_1_1_3000_80	1	1	3003	39.95	7	1	0.00	4	18.02	7	1	81.24
r_1_5_3000_2	1	5	3003	1.03	47	1	0.00	6	0.40	47	1	46.99
r_1_5_3000_4	1	5	3003	2.03	30	1	0.00	4	0.86	30	1	46.24
r_1_5_3000_10	1	5	3003	5.02	14	1	0.00	6	2.14	14	1	48.79
r_1_5_3000_40	1	5	3003	19.99	8	1	0.00	6	9.81	8	1	65.58
r_1_5_3000_80	1	5	3003	39.95	6	1	0.00	4	17.09	6	1	81.79
r_1_10_3000_2	1	10	3003	1.03	37	1	0.00	6	0.45	37	1	47.22
r_1_10_3000_4	1	10	3003	2.03	30	1	0.00	7	1.04	30	1	47.34
r_1_10_3000_10	1	10	3003	5.02	15	1	0.00	6	2.09	15	1	47.74
r_1_10_3000_40	1	10	3003	19.99	8	1	0.00	6	10.26	8	1	66.12
r_1_10_3000_80	1	10	3003	39.95	5	1	0.00	6	20.31	5	1	80.83
r_1_20_3000_2	1	20	3003	1.03	41	1	0.00	6	0.47	41	1	47.37
r_1_20_3000_4	1	20	3003	2.03	28	1	0.00	8	1.10	28	1	46.99
r_1_20_3000_10	1	20	3003	5.02	12	1	0.00	6	2.71	12	1	48.33
r_1_20_3000_40	1	20	3003	19.99	7	1	0.00	10	12.40	7	1	65.27
r_1_20_3000_80	1	20	3003	39.95	4	1	0.00	6	20.59	4	1	81.39
r_5_1_3000_2	5	1	3007	1.03	174	1	0.00	8	0.86	174	1	46.60
r_5_1_3000_4	5	1	3007	2.02	99	1	0.00	8	1.60	99	1	47.21
r_5_1_3000_10	5	1	3007	5.01	57	1	0.00	8	4.48	57	1	46.71
r_5_1_3000_40	5	1	3007	19.94	27	1	0.00	8	16.34	27	1	63.54
r_5_1_3000_80	5	1	3007	39.85	20	1	0.00	8	33.52	20	1	78.86
r_5_5_3000_2	5	5	3007	1.03	138	1	0.00	16	0.99	138	1	45.65
r_5_5_3000_4	5	5	3007	2.02	77	3	0.00	32	3.20	77	3	46.54
r_5_5_3000_10	5	5	3007	5.01	43	1	0.00	32	6.76	43	1	45.39
r_5_5_3000_40	5	5	3007	19.94	21	1	0.00	20	19.87	21	1	63.25
r_5_5_3000_80	5	5	3007	39.85	15	1	0.00	22	43.05	15	1	77.54
r_5_10_3000_2	5	10	3007	1.03	94	1	0.00	35	1.46	94	1	47.55
r_5_10_3000_4	5	10	3007	2.02	72	1	0.00	41	3.01	72	3	47.50
r_5_10_3000_10	5	10	3007	5.01	39	1	0.00	35	7.13	39	1	46.98
r_5_10_3000_40	5	10	3007	19.94	18	1	0.00	40	30.84	18	1	64.29
r_5_10_3000_80	5	10	3007	39.85	15	1	0.00	31	55.84	15	1	78.13
r_5_20_3000_2	5	20	3007	1.03	125	1	0.00	59	1.93	125	1	46.83
r_5_20_3000_4	5	20	3007	2.03	54	1	0.00	32	2.27	54	1	45.66
r_5_20_3000_10	5	20	3007	5.01	36	1	0.00	75	11.06	36	1	46.60
r_5_20_3000_40	5	20	3007	19.94	16	1	0.00	42	29.10	16	1	62.59
r_5_20_3000_80	5	20	3007	39.85	13	1	0.00	33	53.45	13	1	77.99
r_10_1_3000_2	10	1	3012	1.03	357	1	0.00	13	1.15	357	1	47.22
r_10_1_3000_4	10	1	3012	2.02	195	1	0.00	13	2.22	195	1	47.48
r_10_1_3000_10	10	1	3012	4.99	99	1	0.00	13	5.66	99	1	48.19
r_10_1_3000_40	10	1	3012	19.87	51	1	0.00	13	23.81	51	1	66.00
r_10_1_3000_80	10	1	3012	39.72	39	1	0.00	13	53.69	39	1	83.08

(*continued on next page*)

Table 2 (*continued*).

instanceName	nbSet	maxSize	nbNodes	density	BP_value	BP_nodes	BP_gap	BP_cols	BP_cpu	BBnew_value	BBnew_nodes	BBnew_cpu
r_10_5_3000_2	10	5	3012	1.03	256	1	0.00	44	1.84	256	1	47.60
r_10_5_3000_4	10	5	3012	2.02	136	1	0.00	55	3.57	136	1	46.66
r_10_5_3000_10	10	5	3012	4.99	76	1	0.00	40	9.62	76	1	48.35
r_10_5_3000_40	10	5	3012	19.88	39	1	0.00	49	38.25	39	1	65.84
r_10_5_3000_80	10	5	3012	39.72	28	1	0.00	33	73.06	28	1	80.88
r_10_10_3000_2	10	10	3012	1.03	213	1	0.00	54	1.66	213	1	46.86
r_10_10_3000_4	10	10	3012	2.02	132	1	0.00	70	4.47	132	1	47.49
r_10_10_3000_10	10	10	3012	5.00	65	1	0.00	52	10.14	65	1	47.54
r_10_10_3000_40	10	10	3012	19.88	34	1	0.00	55	39.63	34	1	65.70
r_10_10_3000_80	10	10	3012	39.72	26	1	0.00	52	91.55	26	1	81.56
r_10_20_3000_2	10	20	3012	1.03	162	1	0.00	101	3.86	162	1	48.79
r_10_20_3000_4	10	20	3012	2.02	107	1	0.00	115	5.95	107	1	47.33
r_10_20_3000_10	10	20	3012	5.00	56	1	0.00	95	15.86	56	1	48.20
r_10_20_3000_40	10	20	3012	19.88	32	1	0.00	125	72.81	32	1	65.29
r_10_20_3000_80	10	20	3012	39.72	23	1	0.00	113	120.77	−1	0	1800.00
r_20_1_3000_2	20	1	3022	1.02	668	1	0.00	26	2.43	668	1	46.76
r_20_1_3000_4	20	1	3022	2.00	342	1	0.00	29	4.90	342	5	46.88
r_20_1_3000_10	20	1	3022	4.96	196	1	0.00	23	9.53	196	3	48.37
r_20_1_3000_40	20	1	3022	19.74	89	1	0.00	23	48.17	89	3	65.94
r_20_1_3000_80	20	1	3022	39.45	69	1	0.00	25	105.05	69	3	79.78
r_20_5_3000_2	20	5	3022	1.02	441	1	0.00	91	3.28	441	11	46.05
r_20_5_3000_4	20	5	3022	2.01	266	1	0.00	88	7.03	266	1	46.30
r_20_5_3000_10	20	5	3022	4.96	137	1	0.00	69	14.59	137	1	45.98
r_20_5_3000_40	20	5	3022	19.75	67	1	0.00	75	70.39	67	1	63.71
r_20_5_3000_80	20	5	3022	39.45	55	1	0.00	74	144.10	55	1	78.39
r_20_10_3000_2	20	10	3022	1.02	413	1	0.00	123	4.58	413	3	47.25
r_20_10_3000_4	20	10	3022	2.01	236	1	0.00	144	7.77	236	1	47.16
r_20_10_3000_10	20	10	3022	4.96	135	1	0.00	177	25.45	135	3	46.58
r_20_10_3000_40	20	10	3022	19.75	61	1	0.00	88	68.28	61	1	65.38
r_20_10_3000_80	20	10	3022	39.46	45	1	0.00	116	151.69	45	1	80.62
r_20_20_3000_2	20	20	3022	1.03	343	1	0.00	290	8.76	343	11	46.72
r_20_20_3000_4	20	20	3022	2.01	208	11	0.65	384	27.48	208	11	47.24
r_20_20_3000_10	20	20	3022	4.97	104	1	0.00	168	28.26	104	1	47.43
r_20_20_3000_40	20	20	3022	19.75	54	1	0.00	195	121.00	54	1	63.97
r_20_20_3000_80	20	20	3022	39.46	41	1	0.00	160	197.80	41	1	79.50

Table 3
Numerical results comparing the Branch-and-Price and $B\&B^{new}$ algorithms on Literature instances.

instanceName	nbSet	maxSize	nbNodes	density	BP_value	BP_nodes	BP_gap	BP_cols	BP_cpu	BBnew_value	BBnew_nodes	BBnew_cpu
Complete_100N10t35_27000	12	6	110	83.24	186	1	0.00	27	0.12	186	1	0.00
Complete_100N10t35_27001	12	7	110	83.24	173	1	0.00	33	0.12	173	1	0.00
Complete_100N10t35_27002	12	7	110	83.24	187	1	0.00	36	0.14	187	1	0.00
Complete_100N10t35_27003	12	5	110	83.24	173	1	0.00	27	0.12	173	1	0.00
Complete_100N25t35_27001	27	3	125	64.49	603	1	0.00	34	0.21	603	1	0.00
Complete_100N25t35_27002	27	3	125	64.49	630	1	0.00	38	0.23	630	1	0.00
Complete_100N25t35_27003	27	3	125	64.49	578	1	0.00	36	0.23	578	1	0.00
Complete_100N25t35_27004	27	3	125	64.49	592	1	0.00	36	0.21	592	1	0.00
Complete_100N25t35_27005	27	3	125	64.49	627	1	0.00	34	0.22	627	1	0.00
Complete_100N25t35_27006	27	3	125	64.49	622	1	0.00	33	0.24	622	1	0.00
Complete_100N25t35_27007	27	3	125	64.49	623	1	0.00	39	0.23	623	3	0.00
Complete_100N25t35_27008	27	3	125	64.49	635	1	0.00	34	0.23	635	1	0.00
Complete_100N25t35_27009	27	3	125	64.49	607	1	0.00	32	0.23	607	1	0.00
Complete_100N25t70_27000	27	6	125	64.94	527	1	0.00	69	0.32	527	1	0.00
Complete_100N25t70_27001	27	5	125	64.94	506	1	0.00	68	0.32	506	1	0.00
Complete_100N25t70_27002	27	6	125	64.94	529	1	0.00	53	0.28	529	1	0.00
Complete_100N25t70_27003	27	5	125	64.94	521	1	0.00	74	0.33	521	3	0.00
Complete_100N25t70_27004	27	6	125	64.94	516	1	0.00	63	0.32	516	1	0.00
Complete_100N25t70_27005	27	5	125	64.94	515	1	0.00	60	0.30	515	1	0.00
Complete_100N25t70_27006	27	5	125	64.94	526	1	0.00	58	0.29	526	1	0.00
Complete_100N25t70_27007	27	4	125	64.94	504	1	0.00	74	0.33	504	1	0.00
Complete_100N25t70_27008	27	5	125	64.94	538	1	0.00	68	0.35	538	1	0.00
Complete_100N25t70_27009	27	8	125	64.94	499	1	0.00	59	0.33	499	3	0.00
Complete_150N10t35_27000	17	6	165	83.04	298	1	0.00	49	0.42	298	1	0.01
Complete_150N10t35_27001	17	7	165	83.04	271	1	0.00	44	0.42	271	1	0.01
Complete_150N10t35_27002	17	6	165	83.04	284	1	0.00	56	0.42	284	1	0.01
Complete_150N10t35_27003	17	5	165	83.04	275	1	0.00	49	0.38	275	1	0.01
Complete_150N10t35_27004	17	5	165	83.04	279	1	0.00	43	0.40	279	1	0.01
Complete_150N10t35_27005	17	5	165	83.04	252	1	0.00	46	0.40	252	1	0.01
Complete_150N10t35_27006	17	5	165	83.04	317	1	0.00	46	0.42	317	1	0.01
Complete_150N10t35_27007	17	11	165	83.04	290	1	0.00	39	0.40	290	1	0.01
Complete_150N10t35_27008	17	6	165	83.04	307	1	0.00	47	0.44	307	1	0.01
Complete_150N10t35_27009	17	9	165	83.04	288	1	0.00	40	0.37	288	1	0.01

(*continued on next page*)

Table 3 (*continued*).

instanceName	nbSet	maxSize	nbNodes	density	BP_value	BP_nodes	BP_gap	BP_cols	BP_cpu	BBnew_value	BBnew_nodes	BBnew_cpu
Complete_150N10t70_27000	17	12	165	83.43	236	1	0.00	91	0.55	236	1	0.01
Complete_150N10t70_27001	17	13	165	83.43	209	1	0.00	64	0.50	209	1	0.01
Complete_150N10t70_27002	17	11	165	83.43	237	1	0.00	124	0.70	237	1	0.01
Complete_150N10t70_27003	17	11	165	83.43	233	1	0.00	83	0.59	233	1	0.01
Complete_150N10t70_27004	17	10	165	83.43	235	1	0.00	91	0.61	235	1	0.01
Complete_150N10t70_27005	17	12	165	83.43	202	1	0.00	72	0.56	202	1	0.01
Complete_150N10t70_27006	17	10	165	83.43	237	1	0.00	108	0.66	237	1	0.01
Complete_150N10t70_27007	17	15	165	83.43	261	1	0.00	84	0.60	261	1	0.01
Complete_150N10t70_27008	17	12	165	83.43	243	1	0.00	78	0.60	243	1	0.01
Complete_150N10t70_27009	17	12	165	83.43	232	1	0.00	69	0.53	232	1	0.01
Complete_150N25t35_27000	39	3	187	64.67	879	1	0.00	53	0.84	879	1	0.01
Complete_150N25t35_27001	39	3	187	64.67	886	1	0.00	53	0.82	886	1	0.01
Complete_150N25t35_27002	39	3	187	64.67	839	1	0.00	56	0.86	839	1	0.01
Complete_150N25t35_27003	39	4	187	64.67	798	1	0.00	46	0.73	798	1	0.01
Complete_150N25t35_27004	39	3	187	64.67	843	1	0.00	43	0.75	843	1	0.01
Complete_150N25t35_27005	39	3	187	64.67	853	1	0.00	52	0.80	853	1	0.01
Complete_150N25t35_27006	39	4	187	64.67	929	1	0.00	58	0.89	929	1	0.01
Complete_150N25t35_27007	39	3	187	64.67	925	1	0.00	59	0.89	925	1	0.01
Complete_150N25t35_27008	39	3	187	64.67	859	1	0.00	56	0.86	859	7	0.01
Complete_150N25t35_27009	39	4	187	64.67	882	1	0.00	52	0.86	882	1	0.01
Complete_150N25t70_27000	39	7	187	64.97	761	1	0.00	86	1.15	761	1	0.01
Complete_150N25t70_27001	39	5	187	64.97	693	1	0.00	86	1.14	693	3	0.01
Complete_150N25t70_27002	39	6	187	64.97	712	1	0.00	91	1.13	712	1	0.01
Complete_150N25t70_27003	39	7	187	64.97	698	1	0.00	92	1.17	698	1	0.01
Complete_150N25t70_27004	39	7	187	64.97	739	1	0.00	102	1.19	739	1	0.01
Complete_150N25t70_27005	39	6	187	64.97	737	1	0.00	91	1.20	737	1	0.01
Complete_150N25t70_27006	39	5	187	64.97	740	1	0.00	82	1.06	740	1	0.01
Complete_150N25t70_27007	39	8	187	64.97	760	1	0.00	88	1.10	760	1	0.01
Complete_150N25t70_27008	39	6	187	64.97	768	1	0.00	84	1.10	768	1	0.01
Complete_150N25t70_27009	39	7	187	64.97	755	1	0.00	101	1.19	755	3	0.01
Complete_200N10t35_27000	22	7	220	82.94	390	1	0.00	82	1.08	390	1	0.02
Complete_200N10t35_27001	22	8	220	82.94	365	1	0.00	71	0.98	365	1	0.02
Complete_200N10t35_27002	22	7	220	82.94	349	1	0.00	61	0.94	349	1	0.02
Complete_200N10t35_27003	22	6	220	82.94	361	1	0.00	61	1.00	361	3	0.02
Complete_200N10t35_27004	22	6	220	82.94	372	1	0.00	59	0.94	372	1	0.02
Complete_200N10t35_27005	22	7	220	82.94	380	1	0.00	56	0.96	380	1	0.02
Complete_200N10t35_27006	22	6	220	82.94	363	1	0.00	62	1.03	363	1	0.02
Complete_200N10t35_27007	22	6	220	82.94	341	1	0.00	61	0.93	341	1	0.02
Complete_200N10t35_27008	22	8	220	82.94	383	1	0.00	64	0.98	383	1	0.02
Complete_200N10t35_27009	22	5	220	82.94	345	1	0.00	64	0.96	345	1	0.02
Complete_200N10t70_27000	22	10	220	83.23	280	1	0.00	98	1.26	280	1	0.02
Complete_200N10t70_27001	22	12	220	83.23	286	1	0.00	94	1.17	286	1	0.02
Complete_200N10t70_27002	22	10	220	83.23	300	1	0.00	92	1.24	300	1	0.02
Complete_200N10t70_27003	22	12	220	83.23	302	1	0.00	115	1.28	302	1	0.02
Complete_200N10t70_27004	22	14	220	83.23	300	1	0.00	93	1.27	300	1	0.02
Complete_200N10t70_27005	22	11	220	83.23	308	1	0.00	96	1.38	308	1	0.02
Complete_200N10t70_27006	22	12	220	83.23	329	1	0.00	125	1.42	329	1	0.02
Complete_200N10t70_27007	22	12	220	83.23	301	1	0.00	128	1.34	301	1	0.02
Complete_200N10t70_27008	22	14	220	83.23	308	1	0.00	118	1.29	308	1	0.02
Complete_200N10t70_27009	22	13	220	83.23	303	1	0.00	109	1.37	303	1	0.02
Complete_200N25t35_27000	52	3	250	64.24	1164	1	0.00	73	2.15	1164	1	0.02
Complete_200N25t35_27001	52	3	250	64.24	1206	1	0.00	69	2.13	1206	3	0.02
Complete_200N25t35_27002	52	3	250	64.24	1137	1	0.00	78	2.20	1137	7	0.02
Complete_200N25t35_27003	52	3	250	64.24	1198	1	0.00	74	2.21	1198	1	0.02
Complete_200N25t35_27004	52	3	250	64.24	1170	1	0.00	71	2.20	1170	1	0.02
Complete_200N25t35_27005	52	3	250	64.24	1138	1	0.00	72	2.25	1138	1	0.02
Complete_200N25t35_27006	52	3	250	64.24	1170	1	0.00	71	2.15	1170	3	0.02
Complete_200N25t35_27007	52	3	250	64.24	1152	1	0.00	70	2.21	1152	1	0.02
Complete_200N25t35_27008	52	3	250	64.24	1243	1	0.00	71	2.23	1243	3	0.02
Complete_200N25t35_27009	52	3	250	64.24	1151	1	0.00	69	2.18	1151	3	0.02
Complete_200N25t70_27000	52	6	250	64.47	949	1	0.00	102	2.68	949	3	0.02
Complete_200N25t70_27001	52	7	250	64.47	1005	1	0.00	123	2.95	1005	1	0.02
Complete_200N25t70_27002	52	5	250	64.47	976	1	0.00	125	2.88	976	1	0.02
Complete_200N25t70_27003	52	6	250	64.47	992	1	0.00	119	2.88	992	1	0.02
Complete_200N25t70_27004	52	6	250	64.47	1021	1	0.00	132	2.99	1021	1	0.02
Complete_200N25t70_27005	52	6	250	64.47	957	1	0.00	125	2.91	957	1	0.02
Complete_200N25t70_27006	52	6	250	64.47	999	1	0.00	129	2.92	999	3	0.02
Complete_200N25t70_27007	52	8	250	64.47	1025	1	0.00	121	2.83	1025	1	0.02
Complete_200N25t70_27008	52	7	250	64.47	990	1	0.00	131	3.07	990	1	0.02
Complete_200N25t70_27009	52	10	250	64.47	992	1	0.00	119	2.89	992	1	0.02
Complete_250N10t35_27000	27	6	275	82.88	451	1	0.00	72	1.87	451	1	0.04
Complete_250N10t35_27001	27	7	275	82.88	423	1	0.00	58	1.69	423	1	0.04
Complete_250N10t35_27002	27	6	275	82.88	445	1	0.00	70	1.93	445	1	0.04
Complete_250N10t35_27003	27	6	275	82.88	443	1	0.00	81	1.90	443	1	0.04

(*continued on next page*)

Table 3 (*continued*).

instanceName	nbSet	maxSize	nbNodes	density	BP_value	BP_nodes	BP_gap	BP_cols	BP_cpu	BBnew_value	BBnew_nodes	BBnew_cpu
Complete_250N10t35_27004	27	8	275	82.88	433	1	0.00	65	1.77	433	1	0.04
Complete_250N10t35_27005	27	8	275	82.88	483	1	0.00	67	1.97	483	1	0.04
Complete_250N10t35_27006	27	7	275	82.88	462	1	0.00	72	1.83	462	1	0.04
Complete_250N10t35_27007	27	6	275	82.88	422	1	0.00	70	1.93	422	1	0.04
Complete_250N10t35_27008	27	7	275	82.88	461	1	0.00	70	1.85	461	1	0.04
Complete_250N10t35_27009	27	6	275	82.88	467	1	0.00	72	2.06	467	1	0.04
Complete_250N10t70_27000	27	12	275	83.11	384	1	0.00	148	2.46	384	1	0.04
Complete_250N10t70_27001	27	14	275	83.11	372	1	0.00	113	2.31	372	1	0.04
Complete_250N10t70_27002	27	14	275	83.11	368	1	0.00	129	2.42	368	1	0.04
Complete_250N10t70_27003	27	11	275	83.11	369	1	0.00	132	2.42	369	1	0.04
Complete_250N10t70_27004	27	12	275	83.11	382	1	0.00	136	2.35	382	1	0.04
Complete_250N10t70_27005	27	12	275	83.11	405	1	0.00	136	2.50	405	1	0.04
Complete_250N10t70_27006	27	13	275	83.11	391	1	0.00	133	2.46	391	1	0.04
Complete_250N25t35_27007	64	3	312	64.40	1448	1	0.00	93	4.76	1448	3	0.05
Complete_250N25t35_27008	64	3	312	64.40	1424	1	0.00	98	4.90	1424	3	0.04
Complete_250N25t35_27009	64	3	312	64.40	1425	1	0.00	85	4.40	1425	3	0.04
Complete_250N25t70_27000	64	7	312	64.58	1220	1	0.00	145	6.14	1220	3	0.04
Complete_250N25t70_27001	64	7	312	64.58	1200	1	0.00	142	6.24	1200	1	0.04
Complete_250N25t70_27002	64	5	312	64.58	1225	1	0.00	149	5.84	1225	1	0.04
Complete_250N25t70_27003	64	7	312	64.58	1187	1	0.00	149	5.98	1187	1	0.04
Complete_250N25t70_27004	64	6	312	64.58	1231	1	0.00	151	5.81	1231	1	0.04
Complete_250N25t70_27005	64	5	312	64.58	1189	1	0.00	161	6.15	1189	1	0.04
Complete_250N25t70_27006	64	5	312	64.58	1134	1	0.00	144	5.61	1134	1	0.04
Complete_250N25t70_27007	64	6	312	64.58	1177	1	0.00	146	5.87	1177	1	0.04
Complete_250N25t70_27008	64	7	312	64.58	1245	1	0.00	152	5.96	1245	1	0.04
Complete_250N25t70_27009	64	7	312	64.58	1194	1	0.00	158	6.02	1194	3	0.04
Complete_300N10t35_27000	32	7	330	82.84	531	1	0.00	89	3.37	531	1	0.06
Complete_300N10t35_27001	32	7	330	82.84	557	1	0.00	95	3.66	557	1	0.06
Complete_300N10t35_27002	32	6	330	82.84	535	1	0.00	89	3.53	535	1	0.06
Complete_300N10t35_27003	32	6	330	82.84	538	1	0.00	94	3.44	538	1	0.06
Complete_300N10t35_27004	32	10	330	82.84	525	1	0.00	82	3.38	525	1	0.06
Complete_300N10t35_27005	32	6	330	82.84	527	1	0.00	85	3.40	527	9	0.07
Complete_300N10t35_27006	32	6	330	82.84	509	1	0.00	89	3.40	509	1	0.06
Complete_300N10t35_27007	32	5	330	82.84	509	1	0.00	85	3.34	509	1	0.06
Complete_300N10t35_27008	32	7	330	82.84	547	1	0.00	96	3.73	547	1	0.06
Complete_300N10t35_27009	32	7	330	82.84	543	1	0.00	75	3.29	543	1	0.06
Complete_300N10t70_27000	32	13	330	83.04	449	1	0.00	146	4.34	449	1	0.06
Complete_300N10t70_27001	32	11	330	83.04	455	1	0.00	121	4.33	455	1	0.06
Complete_300N10t70_27002	32	13	330	83.04	456	1	0.00	150	4.17	456	1	0.06
Complete_300N10t70_27003	32	12	330	83.04	433	1	0.00	147	4.13	433	1	0.06
Complete_300N10t70_27004	32	14	330	83.04	456	1	0.00	188	4.58	456	1	0.06
Complete_300N10t70_27005	32	12	330	83.04	462	1	0.00	157	4.30	462	1	0.06
Complete_300N10t70_27006	32	11	330	83.04	459	1	0.00	155	4.25	459	1	0.06
Complete_300N10t70_27007	32	12	330	83.04	446	1	0.00	159	4.23	446	1	0.06
Complete_300N10t70_27008	32	13	330	83.04	451	1	0.00	159	4.04	451	1	0.06
Complete_300N10t70_27009	32	13	330	83.04	456	1	0.00	179	4.29	456	1	0.06
Complete_300N25t35_27000	77	3	375	64.16	1644	1	0.00	110	8.68	1644	1	0.06
Complete_300N25t35_27001	77	4	375	64.16	1651	1	0.00	104	8.65	1651	1	0.06
Complete_300N25t35_27002	77	3	375	64.16	1704	1	0.00	106	8.77	1704	1	0.06
Complete_300N25t35_27003	77	5	375	64.16	1702	1	0.00	105	8.57	1702	1	0.06
Complete_300N25t35_27004	77	3	375	64.16	1582	1	0.00	104	8.42	1582	1	0.06
Complete_300N25t35_27005	77	4	375	64.16	1636	1	0.00	96	8.19	1636	3	0.06
Complete_300N25t35_27006	77	3	375	64.16	1697	1	0.00	104	8.37	1697	3	0.06
Complete_300N25t35_27007	77	3	375	64.16	1675	1	0.00	100	8.55	1675	3	0.06
Complete_300N25t35_27008	77	3	375	64.16	1644	1	0.00	100	8.19	1644	1	0.06
Complete_300N25t35_27009	77	3	375	64.16	1678	1	0.00	108	8.88	1678	3	0.06
Complete_300N25t70_27000	77	6	375	64.31	1401	1	0.00	171	10.42	1401	1	0.06
Complete_300N25t70_27001	77	6	375	64.31	1432	1	0.00	186	11.54	1432	3	0.07
Complete_300N25t70_27002	77	6	375	64.31	1458	1	0.00	175	11.35	1458	1	0.06
Complete_300N25t70_27003	77	7	375	64.31	1474	1	0.00	179	11.45	1474	1	0.06
Complete_300N25t70_27004	77	7	375	64.31	1424	1	0.00	177	11.35	1424	1	0.06
Complete_300N25t70_27005	77	7	375	64.31	1485	1	0.00	182	11.40	1485	1	0.06
Complete_300N25t70_27006	77	7	375	64.31	1487	1	0.00	184	11.05	1487	3	0.07
Complete_300N25t70_27007	77	6	375	64.31	1426	1	0.00	182	10.83	1426	3	0.07
Complete_300N25t70_27008	77	7	375	64.31	1429	1	0.00	177	10.98	1429	3	0.07
Complete_300N25t70_27009	77	6	375	64.31	1455	1	0.00	173	11.27	1455	1	0.06
Complete_350N10t35_27000	37	7	385	82.81	621	1	0.00	97	5.28	621	1	0.10
Complete_350N10t35_27001	37	6	385	82.81	646	1	0.00	114	6.10	646	1	0.10
Complete_350N10t35_27002	37	9	385	82.81	653	1	0.00	105	5.99	653	1	0.10
Complete_350N10t35_27003	37	8	385	82.81	650	1	0.00	102	5.67	650	1	0.10
Complete_350N10t35_27004	37	6	385	82.81	598	1	0.00	90	5.20	598	1	0.10
Complete_350N10t35_27005	37	9	385	82.81	596	1	0.00	89	5.74	596	1	0.10
Complete_350N10t35_27006	37	8	385	82.81	613	1	0.00	94	5.77	613	1	0.10
Complete_350N10t35_27007	37	8	385	82.81	606	1	0.00	89	5.53	606	1	0.10

(*continued on next page*)

Table 3 (*continued*).

instanceName	nbSet	maxSize	nbNodes	density	BP_value	BP_nodes	BP_gap	BP_cols	BP_cpu	BBnew_value	BBnew_nodes	BBnew_cpu
Complete_350N10t35_27008	37	6	385	82.81	615	1	0.00	81	5.28	615	1	0.10
Complete_350N10t35_27009	37	7	385	82.81	635	1	0.00	96	6.09	635	1	0.10
Complete_350N10t70_27000	37	14	385	82.98	527	1	0.00	161	6.71	527	1	0.10
Complete_350N10t70_27001	37	15	385	82.98	538	1	0.00	162	7.22	538	3	0.12
Complete_350N10t70_27002	37	15	385	82.98	519	1	0.00	161	6.42	519	1	0.10
Complete_350N10t70_27003	37	11	385	82.98	537	1	0.00	168	6.85	537	1	0.10
Complete_350N10t70_27004	37	13	385	82.98	538	1	0.00	161	7.07	538	1	0.10
Complete_350N10t70_27005	37	13	385	82.98	527	1	0.00	138	6.78	527	1	0.10
Complete_350N10t70_27006	37	13	385	82.98	538	1	0.00	179	7.27	538	1	0.10
Complete_350N10t70_27007	37	14	385	82.98	494	1	0.00	170	6.63	494	1	0.10
Complete_350N10t70_27008	37	12	385	82.98	514	1	0.00	175	6.75	514	1	0.10
Complete_350N10t70_27009	37	12	385	82.98	535	1	0.00	184	7.07	535	1	0.10
Complete_350N25t35_27000	89	4	437	64.28	1927	1	0.00	135	15.28	1927	3	0.10
Complete_350N25t35_27001	89	3	437	64.28	1865	1	0.00	116	14.27	1865	1	0.10
Complete_350N25t35_27002	89	3	437	64.28	1980	1	0.00	122	14.61	1980	3	0.10
Complete_350N25t35_27003	89	3	437	64.28	1910	1	0.00	123	14.70	1910	1	0.10
Complete_350N25t35_27004	89	4	437	64.28	1941	1	0.00	115	14.35	1941	1	0.10
Complete_350N25t35_27005	89	4	437	64.28	1972	1	0.00	125	15.79	1972	3	0.10
Complete_350N25t35_27006	89	4	437	64.28	1952	1	0.00	122	15.25	1952	1	0.10
Complete_350N25t35_27007	89	3	437	64.28	1929	1	0.00	121	14.91	1929	1	0.10
Complete_350N25t35_27008	89	3	437	64.28	1922	1	0.00	119	15.04	1922	1	0.10
Complete_350N25t35_27009	89	3	437	64.28	1885	1	0.00	122	14.76	1885	3	0.10
Complete_350N25t70_27000	89	7	437	64.41	1699	1	0.00	207	19.36	1699	1	0.10
Complete_350N25t70_27001	89	7	437	64.41	1655	1	0.00	215	18.91	1655	1	0.10
Complete_350N25t70_27002	89	7	437	64.41	1640	1	0.00	201	18.10	1640	1	0.10
Complete_350N25t70_27003	89	6	437	64.41	1653	1	0.00	193	18.64	1653	1	0.10
Complete_350N25t70_27004	89	8	437	64.41	1676	1	0.00	193	18.47	1676	1	0.10
Complete_350N25t70_27005	89	6	437	64.41	1658	1	0.00	215	18.87	1658	3	0.10
Complete_350N25t70_27006	89	7	437	64.41	1704	1	0.00	217	19.14	1704	1	0.10
Complete_350N25t70_27007	89	8	437	64.41	1635	1	0.00	227	18.36	1635	19	0.19
Complete_350N25t70_27008	89	6	437	64.41	1709	1	0.00	201	19.52	1709	1	0.10
Complete_350N25t70_27009	89	6	437	64.41	1680	1	0.00	210	19.14	1680	3	0.10
Complete_400N10t35_27000	42	7	440	82.79	689	1	0.00	110	8.71	689	1	0.14
Complete_400N10t35_27001	42	7	440	82.79	714	1	0.00	129	9.46	714	1	0.14
Complete_400N10t35_27002	42	7	440	82.79	731	1	0.00	104	8.84	731	1	0.14
Complete_400N10t35_27003	42	6	440	82.79	698	1	0.00	107	8.67	698	1	0.14
Complete_400N10t35_27004	42	9	440	82.79	736	1	0.00	101	9.00	736	1	0.14
Complete_400N10t35_27005	42	7	440	82.79	747	1	0.00	134	9.40	747	1	0.14
Complete_400N10t35_27006	42	8	440	82.79	683	1	0.00	110	8.69	683	1	0.14
Complete_400N10t35_27007	42	8	440	82.79	746	1	0.00	120	9.10	746	1	0.14
Complete_400N10t35_27008	42	12	440	82.79	723	1	0.00	99	8.97	723	1	0.14
Complete_400N10t35_27009	42	7	440	82.79	763	1	0.00	124	9.29	763	1	0.14
Complete_400N10t70_27000	42	10	440	82.94	591	1	0.00	183	11.33	591	1	0.14
Complete_400N10t70_27001	42	15	440	82.94	572	1	0.00	187	10.84	572	1	0.14
Complete_400N10t70_27002	42	13	440	82.94	591	1	0.00	178	10.68	591	1	0.14
Complete_400N10t70_27003	42	13	440	82.94	593	1	0.00	172	11.23	593	1	0.14
Complete_400N10t70_27004	42	17	440	82.94	618	1	0.00	167	10.99	618	1	0.14
Complete_400N10t70_27005	42	14	440	82.94	606	1	0.00	180	11.07	606	1	0.14
Complete_400N10t70_27006	42	12	440	82.94	583	1	0.00	173	11.06	583	1	0.14
Complete_400N10t70_27007	42	12	440	82.94	576	1	0.00	173	10.42	576	1	0.14
Complete_400N10t70_27008	42	14	440	82.94	598	1	0.00	196	10.44	598	1	0.14
Complete_400N10t70_27009	42	14	440	82.94	584	1	0.00	172	9.82	584	1	0.14
Complete_400N25t35_27000	102	4	500	64.12	2187	1	0.00	135	24.77	2187	1	0.14
Complete_400N25t35_27001	102	4	500	64.12	2232	1	0.00	134	26.00	2232	3	0.14
Complete_400N25t35_27002	102	5	500	64.12	2184	1	0.00	133	24.81	2184	3	0.14
Complete_400N25t35_27003	102	4	500	64.12	2198	1	0.00	145	25.92	2198	7	0.17
Complete_400N25t35_27004	102	3	500	64.12	2210	1	0.00	147	25.25	2210	1	0.14
Complete_400N25t35_27005	102	3	500	64.12	2156	1	0.00	135	24.37	2156	3	0.15
Complete_400N25t35_27006	102	4	500	64.12	2211	1	0.00	133	24.17	2211	7	0.15
Complete_400N25t35_27007	102	4	500	64.12	2249	1	0.00	135	25.57	2249	1	0.14
Complete_400N25t35_27008	102	6	500	64.12	2207	1	0.00	148	26.01	2207	3	0.15
Complete_400N25t35_27009	102	4	500	64.12	2244	1	0.00	142	26.28	2244	3	0.14
Complete_400N25t70_27000	102	6	500	64.23	1896	1	0.00	237	32.14	1896	1	0.14
Complete_400N25t70_27001	102	8	500	64.23	1947	1	0.00	257	33.50	1947	1	0.14
Complete_400N25t70_27002	102	6	500	64.23	1930	1	0.00	232	31.38	1930	3	0.15
Complete_400N25t70_27003	102	6	500	64.23	1877	1	0.00	239	32.33	1877	1	0.14
Complete_400N25t70_27004	102	8	500	64.23	1883	1	0.00	258	33.24	1883	1	0.14
Complete_400N25t70_27005	102	7	500	64.23	1962	1	0.00	232	33.02	1962	3	0.15
Complete_400N25t70_27006	102	7	500	64.23	1963	1	0.00	247	33.12	1963	3	0.16
Complete_400N25t70_27007	102	7	500	64.23	1916	1	0.00	222	31.46	1916	1	0.14
Complete_400N25t70_27008	102	7	500	64.23	1897	1	0.00	233	32.61	1897	1	0.14
Complete_400N25t70_27009	102	7	500	64.23	1945	1	0.00	255	34.19	1945	1	0.14
Complete_450N10t35_27000	47	7	495	82.78	810	1	0.00	125	14.45	810	1	0.19
Complete_450N10t35_27001	47	7	495	82.78	768	1	0.00	112	13.73	768	1	0.19
Complete_450N10t35_27002	47	8	495	82.78	786	1	0.00	113	14.74	786	1	0.19

(*continued on next page*)

Table 3 (*continued*).

instanceName	nbSet	maxSize	nbNodes	density	BP_value	BP_nodes	BP_gap	BP_cols	BP_cpu	BBnew_value	BBnew_nodes	BBnew_cpu
Complete_450N10t35_27003	47	6	495	82.78	783	1	0.00	119	14.80	783	1	0.19
Complete_450N10t35_27004	47	8	495	82.78	797	1	0.00	110	14.37	797	1	0.19
Complete_450N10t35_27005	47	7	495	82.78	802	1	0.00	125	14.78	802	1	0.19
Complete_450N10t35_27006	47	8	495	82.78	819	1	0.00	132	14.41	819	1	0.19
Complete_450N10t35_27007	47	7	495	82.78	755	1	0.00	110	13.57	755	1	0.19
Complete_450N10t35_27008	47	8	495	82.78	788	1	0.00	132	13.97	788	1	0.19
Complete_450N10t35_27009	47	8	495	82.78	763	1	0.00	123	14.25	763	1	0.19
Complete_450N10t70_27000	47	12	495	82.90	688	1	0.00	234	17.74	688	1	0.20
Complete_450N10t70_27001	47	13	495	82.90	677	1	0.00	224	17.84	677	1	0.20
Complete_450N10t70_27002	47	12	495	82.90	684	1	0.00	245	17.26	684	1	0.20
Complete_450N10t70_27003	47	12	495	82.90	640	1	0.00	206	17.37	640	1	0.20
Complete_450N10t70_27004	47	12	495	82.90	705	1	0.00	198	16.97	705	1	0.19
Complete_450N10t70_27005	47	12	495	82.90	689	1	0.00	204	16.71	689	1	0.19
Complete_450N10t70_27006	47	12	495	82.90	660	1	0.00	238	17.75	660	1	0.19
Complete_450N10t70_27007	47	12	495	82.90	664	1	0.00	228	16.75	664	1	0.19
Complete_450N10t70_27008	47	13	495	82.90	692	1	0.00	205	17.39	692	1	0.19
Complete_450N10t70_27009	47	13	495	82.90	651	1	0.00	187	16.69	651	1	0.19
Complete_450N25t35_27000	114	5	562	64.22	2423	1	0.00	153	45.44	2423	3	0.21
Complete_450N25t35_27001	114	3	562	64.22	2399	1	0.00	153	44.85	2399	3	0.20
Complete_450N25t35_27002	114	3	562	64.22	2388	1	0.00	153	44.43	2388	1	0.19
Complete_450N25t35_27003	114	4	562	64.22	2442	1	0.00	158	44.30	2442	3	0.20
Complete_450N25t35_27004	114	3	562	64.22	2440	1	0.00	152	44.79	2440	1	0.19
Complete_450N25t35_27005	114	4	562	64.22	2400	1	0.00	155	43.92	2400	1	0.19
Complete_450N25t35_27006	114	4	562	64.22	2478	1	0.00	157	46.18	2478	3	0.21
Complete_450N25t35_27007	114	4	562	64.22	2456	1	0.00	155	46.34	2456	3	0.20
Complete_450N25t35_27008	114	4	562	64.22	2440	1	0.00	152	44.73	2440	3	0.20
Complete_450N25t35_27009	114	3	562	64.22	2464	1	0.00	151	45.07	2464	3	0.20
Complete_450N25t70_27000	114	8	562	64.32	2107	1	0.00	260	56.75	2107	1	0.19
Complete_450N25t70_27001	114	6	562	64.32	2101	1	0.00	257	55.72	2101	1	0.19
Complete_450N25t70_27002	114	7	562	64.32	2067	1	0.00	261	54.91	2067	1	0.19
Complete_450N25t70_27003	114	8	562	64.32	2153	1	0.00	248	56.06	2153	1	0.19
Complete_450N25t70_27004	114	8	562	64.32	2161	1	0.00	273	57.15	2161	1	0.19
Complete_450N25t70_27005	114	6	562	64.32	2164	1	0.00	285	57.37	2164	1	0.20
Complete_450N25t70_27006	114	7	562	64.32	2091	1	0.00	275	56.49	2091	1	0.20
Complete_450N25t70_27007	114	7	562	64.32	2139	1	0.00	260	55.60	2139	1	0.20
Complete_450N25t70_27008	114	7	562	64.32	2138	1	0.00	257	56.53	2138	1	0.20
Complete_450N25t70_27009	114	7	562	64.32	2050	1	0.00	251	54.95	2050	1	0.20
Complete_500N10t35_27000	52	7	550	82.76	929	1	0.00	141	21.35	929	1	0.27
Complete_500N10t35_27001	52	8	550	82.76	828	1	0.00	127	20.08	828	1	0.27
Complete_500N10t35_27002	52	7	550	82.76	862	1	0.00	122	20.36	862	1	0.27
Complete_500N10t35_27003	52	8	550	82.76	848	1	0.00	142	20.77	848	1	0.27
Complete_500N10t35_27004	52	8	550	82.76	860	1	0.00	137	21.63	860	1	0.27
Complete_500N10t35_27005	52	9	550	82.76	909	1	0.00	148	21.88	909	3	0.30
Complete_500N10t35_27006	52	9	550	82.76	881	1	0.00	146	21.69	881	1	0.27
Complete_500N10t35_27007	52	9	550	82.76	863	1	0.00	136	21.53	863	1	0.26
Complete_500N10t35_27008	52	7	550	82.76	906	1	0.00	151	22.37	906	3	0.30
Complete_500N10t35_27009	52	6	550	82.76	875	1	0.00	123	21.11	875	1	0.26
Complete_500N10t70_27000	52	14	550	82.88	756	1	0.00	220	24.80	756	1	0.27
Complete_500N10t70_27001	52	13	550	82.88	741	1	0.00	247	25.14	741	1	0.27
Complete_500N10t70_27002	52	14	550	82.88	733	1	0.00	230	26.01	733	1	0.27
Complete_500N10t70_27003	52	12	550	82.88	739	1	0.00	245	26.38	739	1	0.27
Complete_500N10t70_27004	52	15	550	82.88	737	1	0.00	211	24.49	737	1	0.27
Complete_500N10t70_27005	52	14	550	82.88	745	1	0.00	250	26.15	745	1	0.27
Complete_500N10t70_27006	52	17	550	82.88	731	1	0.00	251	24.43	731	1	0.27
Complete_500N10t70_27007	52	14	550	82.88	747	1	0.00	239	26.09	747	1	0.27
Complete_500N10t70_27008	52	12	550	82.88	752	1	0.00	222	24.65	752	1	0.27
Complete_500N10t70_27009	52	12	550	82.88	742	1	0.00	218	23.92	742	1	0.27
Complete_500N25t35_27000	127	4	625	64.10	2727	1	0.00	154	66.36	2727	1	0.26
Complete_500N25t35_27001	127	4	625	64.10	2712	1	0.00	172	70.07	2712	1	0.26
Complete_500N25t35_27002	127	3	625	64.10	2643	1	0.00	174	69.64	2643	1	0.27
Complete_500N25t35_27003	127	4	625	64.10	2648	1	0.00	163	67.56	2648	3	0.28
Complete_500N25t35_27004	127	4	625	64.10	2619	1	0.00	174	67.60	2619	1	0.26
Complete_500N25t35_27005	127	4	625	64.10	2718	1	0.00	169	69.63	2718	3	0.27
Complete_500N25t35_27006	127	3	625	64.10	2704	1	0.00	174	70.18	2704	3	0.28
Complete_500N25t35_27007	127	4	625	64.10	2707	1	0.00	185	72.31	2707	1	0.27
Complete_500N25t35_27008	127	3	625	64.10	2758	1	0.00	182	71.97	2758	3	0.28
Complete_500N25t35_27009	127	3	625	64.10	2657	1	0.00	176	71.23	2657	15	0.31
Complete_500N25t70_27000	127	8	625	64.19	2396	1	0.00	274	86.23	2396	1	0.27
Complete_500N25t70_27001	127	7	625	64.19	2388	1	0.00	280	84.38	2388	3	0.29
Complete_500N25t70_27002	127	8	625	64.19	2346	1	0.00	287	80.48	2346	1	0.27
Complete_500N25t70_27003	127	9	625	64.19	2376	1	0.00	289	80.85	2376	1	0.26
Complete_500N25t70_27004	127	7	625	64.19	2278	1	0.00	281	83.93	2278	1	0.26
Complete_500N25t70_27005	127	7	625	64.19	2330	1	0.00	314	87.68	2330	3	0.27
Complete_500N25t70_27006	127	6	625	64.19	2319	1	0.00	295	85.95	2319	7	0.31
Complete_500N25t70_27007	127	7	625	64.19	2424	1	0.00	324	72.18	2424	1	0.27

(*continued on next page*)

Table 3 (*continued*).

instanceName	nbSet	maxSize	nbNodes	density	BP_value	BP_nodes	BP_gap	BP_cols	BP_cpu	BBnew_value	BBnew_nodes	BBnew_cpu
Complete_500N25t70_27008	127	6	625	64.19	2345	1	0.00	303	76.41	2345	1	0.27
Complete_500N25t70_27009	127	6	625	64.19	2356	1	0.00	295	77.17	2356	3	0.31
Grid_10 × 10N10t35_27000	12	7	110	3.68	1320	1	0.00	37	0.02	1320	1	0.00
Grid_10 × 10N10t35_27001	12	8	110	3.68	1389	1	0.00	37	0.02	1389	1	0.00
Grid_10 × 10N10t35_27002	12	7	110	3.68	1373	1	0.00	46	0.01	1373	3	0.00
Grid_10 × 10N10t35_27003	12	7	110	3.68	1346	1	0.00	43	0.02	1346	19	0.00
Grid_10 × 10N10t35_27004	12	6	110	3.68	1868	27	0.88	89	0.09	1868	95	0.01
Grid_10 × 10N10t35_27005	12	6	110	3.68	1792	1	0.00	60	0.02	1792	13	0.00
Grid_10 × 10N10t35_27006	12	6	110	3.68	1442	1	0.00	28	0.01	1442	1	0.00
Grid_10 × 10N10t35_27007	12	7	110	3.68	1679	1	0.00	44	0.02	1679	13	0.00
Grid_10 × 10N10t35_27008	12	5	110	3.68	1343	15	0.60	63	0.04	1343	173	0.01
Grid_10 × 10N10t35_27009	12	6	110	3.68	1415	7	2.17	62	0.03	1415	7	0.00
Grid_10 × 10N10t70_27000	12	12	110	4.26	939	1	0.00	85	0.05	939	19	0.00
Grid_10 × 10N10t70_27001	12	12	110	4.26	819	1	0.00	59	0.04	819	7	0.00
Grid_10 × 10N10t70_27002	12	11	110	4.26	1041	1	0.00	88	0.05	1041	9	0.00
Grid_10 × 10N10t70_27003	12	10	110	4.26	983	1	0.00	88	0.06	983	5	0.00
Grid_10 × 10N10t70_27004	12	11	110	4.26	858	1	0.00	59	0.04	858	3	0.00
Grid_10 × 10N10t70_27005	12	10	110	4.26	991	1	0.00	81	0.05	991	1	0.00
Grid_10 × 10N10t70_27006	12	15	110	4.26	994	1	0.00	92	0.06	994	7	0.00
Grid_10 × 10N10t70_27007	12	11	110	4.26	946	1	0.00	70	0.05	946	3	0.00
Grid_10 × 10N10t70_27008	12	9	110	4.26	1030	1	0.00	56	0.04	1030	41	0.01
Grid_10 × 10N10t70_27009	12	10	110	4.26	984	1	0.00	82	0.04	984	7	0.00
Grid_10 × 10N25t35_27006	27	3	125	2.94	5781	1	0.00	141	0.04	5781	1 233 003	49.24
Grid_10 × 10N25t70_27000	27	6	125	3.39	4251	15	0.77	219	0.19	4251	778 311	43.74
Grid_10 × 10N25t70_27001	27	5	125	3.39	4395	1	0.00	162	0.09	4395	2 714 569	290.71
Grid_10 × 10N25t70_27002	27	5	125	3.39	4617	29	0.58	233	0.32	4617	2 308 701	187.75
Grid_10 × 10N25t70_27003	27	7	125	3.39	4868	55	0.97	271	0.50	4868	14 004 501	717.24
Grid_10 × 10N25t70_27004	27	8	125	3.39	3782	141	0.40	278	0.88	3782	41 067	1.83
Grid_10 × 10N25t70_27005	27	7	125	3.39	4328	69	0.74	269	0.56	4328	82 073	5.22
Grid_10 × 10N25t70_27006	27	8	125	3.39	3812	1	0.00	147	0.09	3812	15 215	0.75
Grid_10 × 10N25t70_27007	27	5	125	3.39	4428	1	0.00	121	0.08	4428	16 027	0.74
Grid_10 × 10N25t70_27009	27	6	125	3.39	4690	1	0.00	115	0.09	4690	14 985	0.65
Grid_10 × 20N10t35_27000	22	6	220	1.87	4896	1	0.00	118	0.09	4896	2063	0.33
Grid_10 × 20N10t35_27001	22	9	220	1.87	3973	1	0.00	90	0.09	3973	1295	0.19
Grid_10 × 20N10t35_27002	22	7	220	1.87	4294	1	0.00	106	0.08	4294	1029	0.21
Grid_10 × 20N10t35_27003	22	6	220	1.87	3524	1	0.00	90	0.07	3524	27	0.01
Grid_10 × 20N10t35_27004	22	6	220	1.87	3435	3	1.12	170	0.12	3435	1799	0.33
Grid_10 × 20N10t35_27005	22	6	220	1.87	3006	1	0.00	102	0.08	3006	7733	1.51
Grid_10 × 20N10t35_27006	22	6	220	1.87	3007	1	0.00	87	0.08	3007	19	0.01
Grid_10 × 20N10t35_27007	22	6	220	1.87	3423	1	0.00	134	0.09	3423	1115	0.11
Grid_10 × 20N10t35_27008	22	6	220	1.87	3807	1	0.00	129	0.08	3807	1459	0.24
Grid_10 × 20N10t35_27009	22	7	220	1.87	4231	1	0.00	122	0.08	4231	3037	0.47
Grid_10 × 20N10t70_27000	22	10	220	2.16	2903	5	0.05	200	0.33	2903	19	0.02
Grid_10 × 20N10t70_27001	22	14	220	2.16	2763	17	1.08	244	0.69	2763	335	0.12
Grid_10 × 20N10t70_27002	22	14	220	2.16	2981	13	1.36	285	0.64	2981	2785	0.77
Grid_10 × 20N10t70_27003	22	14	220	2.16	2289	1	0.00	114	0.26	2289	13	0.01
Grid_10 × 20N10t70_27004	22	12	220	2.16	2198	1	0.00	176	0.25	2198	33	0.02
Grid_10 × 20N10t70_27005	22	10	220	2.16	2287	27	0.44	263	0.69	2287	99	0.05
Grid_10 × 20N10t70_27006	22	12	220	2.16	2299	1	0.00	151	0.27	2299	7	0.01
Grid_10 × 20N10t70_27007	22	12	220	2.16	2538	7	0.03	246	0.45	2538	2731	1.65
Grid_10 × 20N10t70_27008	22	12	220	2.16	2842	151	2.07	321	2.49	2842	185	0.09
Grid_10 × 20N10t70_27009	22	12	220	2.16	2661	1	0.00	141	0.29	2661	23	0.02
Grid_15 × 15N10t35_27000	24	6	247	1.68	4885	1	0.00	123	0.09	4885	2857	0.60
Grid_15 × 15N10t35_27001	24	6	247	1.68	4950	25	0.49	194	0.28	4950	7503	1.25
Grid_15 × 15N10t35_27002	24	8	247	1.68	5265	1	0.00	120	0.10	5265	51	0.02
Grid_15 × 15N10t35_27003	24	7	247	1.68	5722	1	0.00	170	0.12	5722	3 635 223	607.77
Grid_15 × 15N10t35_27005	24	6	247	1.68	4399	1	0.00	127	0.10	4399	367	0.09
Grid_15 × 15N10t35_27006	24	7	247	1.68	4168	1	0.00	114	0.09	4168	55	0.02
Grid_15 × 15N10t35_27007	24	7	247	1.68	4843	5	0.17	165	0.16	4843	2973	0.77
Grid_15 × 15N10t35_27008	24	7	247	1.68	4312	1	0.00	135	0.10	4312	427	0.09
Grid_15 × 15N10t35_27009	24	6	247	1.68	4719	3	0.15	127	0.11	4719	729	0.14
Grid_15 × 15N10t70_27000	24	12	247	1.94	3116	11	1.05	261	0.63	3116	135	0.09
Grid_15 × 15N10t70_27001	24	11	247	1.94	2920	7	0.31	208	0.45	2920	45	0.03
Grid_15 × 15N10t70_27002	24	11	247	1.94	3034	1	0.00	203	0.29	3034	7	0.02
Grid_15 × 15N10t70_27003	24	13	247	1.94	3512	11	0.29	339	0.73	3512	43 401	30.98
Grid_15 × 15N10t70_27004	24	11	247	1.94	2844	1	0.00	174	0.28	2844	17	0.02
Grid_15 × 15N10t70_27005	24	12	247	1.94	2839	1	0.00	166	0.30	2839	47	0.02
Grid_15 × 15N10t70_27006	24	12	247	1.94	3073	1	0.00	150	0.32	3073	15	0.02
Grid_15 × 15N10t70_27007	24	15	247	1.94	3251	1	0.00	167	0.33	3251	19	0.02
Grid_15 × 15N10t70_27008	24	11	247	1.94	2838	1	0.00	171	0.30	2838	7	0.02
Grid_15 × 15N10t70_27009	24	13	247	1.94	3338	1	0.00	236	0.35	3338	15	0.02
Grid_15 × 30N10t70_27004	47	11	495	0.98	8483	3	0.06	490	2.62	8483	782 085	853.41
Grid_5 × 10N10t35_27000	7	6	55	7.07	549	1	0.00	26	0.01	549	3	0.00

(*continued on next page*)

Table 3 (*continued*).

instanceName	nbSet	maxSize	nbNodes	density	BP_value	BP_nodes	BP_gap	BP_cols	BP_cpu	BBnew_value	BBnew_nodes	BBnew_cpu
Grid_5 × 10N10t35_27001	7	5	55	7.07	892	1	0.00	25	0.01	892	3	0.00
Grid_5 × 10N10t35_27002	7	4	55	7.07	358	1	0.00	16	0.00	358	1	0.00
Grid_5 × 10N10t35_27003	7	5	55	7.07	608	1	0.00	22	0.01	608	1	0.00
Grid_5 × 10N10t35_27004	7	6	55	7.07	557	1	0.00	12	0.00	557	1	0.00
Grid_5 × 10N10t35_27005	7	4	55	7.07	414	1	0.00	14	0.00	414	1	0.00
Grid_5 × 10N10t35_27006	7	5	55	7.07	443	1	0.00	17	0.00	443	1	0.00
Grid_5 × 10N10t35_27007	7	7	55	7.07	655	1	0.00	18	0.00	655	1	0.00
Grid_5 × 10N10t35_27008	7	5	55	7.07	562	1	0.00	27	0.01	562	1	0.00
Grid_5 × 10N10t35_27009	7	4	55	7.07	398	1	0.00	16	0.00	398	1	0.00
Grid_5 × 10N10t70_27000	7	10	55	8.28	261	1	0.00	37	0.01	261	1	0.00
Grid_5 × 10N10t70_27001	7	13	55	8.28	632	1	0.00	34	0.01	632	5	0.00
Grid_5 × 10N10t70_27002	7	9	55	8.28	310	1	0.00	26	0.01	310	1	0.00
Grid_5 × 10N10t70_27003	7	9	55	8.28	336	1	0.00	33	0.01	336	1	0.00
Grid_5 × 10N10t70_27004	7	12	55	8.28	557	1	0.00	42	0.01	557	1	0.00
Grid_5 × 10N10t70_27005	7	13	55	8.28	414	1	0.00	24	0.01	414	1	0.00
Grid_5 × 10N10t70_27006	7	12	55	8.28	294	1	0.00	22	0.01	294	1	0.00
Grid_5 × 10N10t70_27007	7	12	55	8.28	241	1	0.00	25	0.01	241	1	0.00
Grid_5 × 10N10t70_27008	7	10	55	8.28	430	1	0.00	40	0.01	430	1	0.00
Grid_5 × 10N10t70_27009	7	9	55	8.28	287	1	0.00	27	0.01	287	1	0.00
Grid_5 × 10N25t35_27000	14	2	62	5.74	2223	1	0.00	61	0.01	2223	95 807	1.98
Grid_5 × 10N25t35_27001	14	2	62	5.74	2112	1	0.00	31	0.01	2112	85	0.00
Grid_5 × 10N25t35_27002	14	2	62	5.74	1870	1	0.00	24	0.01	1870	19	0.00
Grid_5 × 10N25t35_27003	14	3	62	5.74	2680	1	0.00	79	0.01	2680	15 523	0.19
Grid_5 × 10N25t35_27004	14	3	62	5.74	2243	1	0.00	46	0.01	2243	2863	0.05
Grid_5 × 10N25t35_27005	14	3	62	5.74	2475	3	0.14	49	0.01	2475	169	0.00
Grid_5 × 10N25t35_27006	14	3	62	5.74	2611	1	0.00	31	0.01	2611	59	0.00
Grid_5 × 10N25t35_27007	14	2	62	5.74	2193	1	0.00	26	0.01	2193	41	0.00
Grid_5 × 10N25t35_27008	14	3	62	5.74	1738	1	0.00	29	0.01	1738	9	0.00
Grid_5 × 10N25t35_27009	14	3	62	5.74	2606	1	0.00	49	0.01	2606	2881	0.05
Grid_5 × 10N25t70_27000	14	6	62	6.69	1271	1	0.00	40	0.01	1271	123	0.00
Grid_5 × 10N25t70_27001	14	6	62	6.69	1606	1	0.00	39	0.01	1606	1	0.00
Grid_5 × 10N25t70_27002	14	6	62	6.69	1401	1	0.00	37	0.01	1401	7	0.00
Grid_5 × 10N25t70_27003	14	5	62	6.69	1213	1	0.00	46	0.01	1213	37	0.00
Grid_5 × 10N25t70_27004	14	7	62	6.69	1524	1	0.00	49	0.01	1524	43	0.00
Grid_5 × 10N25t70_27005	14	5	62	6.69	1501	1	0.00	52	0.01	1501	31	0.00
Grid_5 × 10N25t70_27006	14	6	62	6.69	1223	1	0.00	38	0.01	1223	1	0.00
Grid_5 × 10N25t70_27007	14	6	62	6.69	1351	1	0.00	33	0.01	1351	11	0.00
Grid_5 × 10N25t70_27008	14	5	62	6.69	1245	1	0.00	29	0.01	1245	1	0.00
Grid_5 × 10N25t70_27009	14	5	62	6.69	1727	1	0.00	61	0.01	1727	87	0.00
Grid_5 × 5N10t35_27000	4	7	27	14.10	53	1	0.00	9	0.00	53	1	0.00
Grid_5 × 5N10t35_27001	4	7	27	14.10	222	1	0.00	7	0.00	222	1	0.00
Grid_5 × 5N10t35_27002	4	7	27	14.10	117	1	0.00	6	0.00	117	1	0.00
Grid_5 × 5N10t35_27003	4	7	27	14.10	66	1	0.00	3	0.00	66	1	0.00
Grid_5 × 5N10t35_27004	4	7	27	14.10	138	1	0.00	7	0.00	138	1	0.00
Grid_5 × 5N10t35_27005	4	7	27	14.10	49	1	0.00	3	0.00	49	1	0.00
Grid_5 × 5N10t35_27006	4	7	27	14.10	161	1	0.00	9	0.00	161	1	0.00
Grid_5 × 5N10t35_27007	4	7	27	14.10	48	1	0.00	7	0.00	48	1	0.00
Grid_5 × 5N10t35_27008	4	7	27	14.10	181	1	0.00	6	0.00	181	1	0.00
Grid_5 × 5N10t35_27009	4	7	27	14.10	141	1	0.00	5	0.00	141	1	0.00
Grid_5 × 5N10t70_27000	4	16	27	16.67	53	1	0.00	6	0.00	53	1	0.00
Grid_5 × 5N10t70_27001	4	16	27	16.67	222	1	0.00	10	0.00	222	1	0.00
Grid_5 × 5N10t70_27002	4	16	27	16.67	117	1	0.00	8	0.00	117	1	0.00
Grid_5 × 5N10t70_27003	4	16	27	16.67	66	1	0.00	3	0.00	66	1	0.00
Grid_5 × 5N10t70_27004	4	16	27	16.67	138	1	0.00	7	0.00	138	1	0.00
Grid_5 × 5N10t70_27005	4	16	27	16.67	49	1	0.00	5	0.00	49	1	0.00
Grid_5 × 5N10t70_27006	4	16	27	16.67	161	1	0.00	13	0.00	161	1	0.00
Grid_5 × 5N10t70_27007	4	16	27	16.67	48	1	0.00	7	0.00	48	1	0.00
Grid_5 × 5N10t70_27008	4	16	27	16.67	181	1	0.00	13	0.00	181	1	0.00
Grid_5 × 5N10t70_27009	4	16	27	16.67	141	1	0.00	7	0.00	141	1	0.00
Grid_5 × 5N25t35_27000	8	2	31	11.08	480	1	0.00	12	0.00	480	3	0.00
Grid_5 × 5N25t35_27001	8	3	31	11.08	756	1	0.00	10	0.00	756	3	0.00
Grid_5 × 5N25t35_27002	8	2	31	11.08	648	1	0.00	9	0.00	648	1	0.00
Grid_5 × 5N25t35_27003	8	2	31	11.08	810	1	0.00	13	0.00	810	3	0.00
Grid_5 × 5N25t35_27004	8	2	31	11.08	671	1	0.00	12	0.00	671	7	0.00
Grid_5 × 5N25t35_27005	8	2	31	11.08	566	1	0.00	9	0.00	566	1	0.00
Grid_5 × 5N25t35_27006	8	2	31	11.08	670	1	0.00	10	0.00	670	3	0.00
Grid_5 × 5N25t35_27007	8	2	31	11.08	478	1	0.00	11	0.00	478	5	0.00
Grid_5 × 5N25t35_27008	8	2	31	11.08	718	1	0.00	11	0.00	718	1	0.00
Grid_5 × 5N25t35_27009	8	3	31	11.08	728	1	0.00	9	0.00	728	5	0.00
Grid_5 × 5N25t70_27000	8	4	31	13.01	455	1	0.00	31	0.01	455	3	0.00
Grid_5 × 5N25t70_27001	8	5	31	13.01	640	1	0.00	21	0.00	640	7	0.00
Grid_5 × 5N25t70_27002	8	5	31	13.01	648	1	0.00	23	0.00	648	1	0.00
Grid_5 × 5N25t70_27003	8	6	31	13.01	696	1	0.00	17	0.00	696	1	0.00

(*continued on next page*)

Table 3 (*continued*).

instanceName	nbSet	maxSize	nbNodes	density	BP_value	BP_nodes	BP_gap	BP_cols	BP_cpu	BBnew_value	BBnew_nodes	BBnew_cpu
Grid_5 × 5N25t70_27004	8	4	31	13.01	520	1	0.00	22	0.00	520	1	0.00
Grid_5 × 5N25t70_27005	8	4	31	13.01	437	1	0.00	16	0.00	437	1	0.00
Grid_5 × 5N25t70_27006	8	6	31	13.01	511	1	0.00	22	0.00	511	1	0.00
Grid_5 × 5N25t70_27007	8	5	31	13.01	478	1	0.00	24	0.00	478	7	0.00
Grid_5 × 5N25t70_27008	8	5	31	13.01	330	1	0.00	13	0.00	330	1	0.00
Grid_5 × 5N25t70_27009	8	4	31	13.01	694	1	0.00	27	0.01	694	7	0.00
Random_250 × 12450N10t10_27000	27	1	275	16.62	1039	1	0.00	26	0.25	1039	1	0.03
Random_250 × 12450N10t10_27001	27	1	275	16.62	1039	1	0.00	26	0.25	1039	1	0.03
Random_250 × 12450N10t10_27002	27	1	275	16.62	1039	1	0.00	26	0.26	1039	1	0.03
Random_250 × 12450N10t10_27003	27	1	275	16.62	1039	1	0.00	26	0.26	1039	1	0.03
Random_250 × 12450N10t10_27004	27	1	275	16.62	1039	1	0.00	26	0.26	1039	1	0.03
Random_250 × 12450N10t10_27005	27	1	275	16.62	1039	1	0.00	26	0.25	1039	1	0.03
Random_250 × 12450N10t10_27006	27	1	275	16.62	1039	1	0.00	26	0.26	1039	1	0.03
Random_250 × 12450N10t10_27007	27	1	275	16.62	1039	1	0.00	26	0.26	1039	1	0.03
Random_250 × 12450N10t10_27008	27	1	275	16.62	1039	1	0.00	26	0.25	1039	1	0.03
Random_250 × 12450N10t10_27009	27	1	275	16.62	1039	1	0.00	26	0.26	1039	1	0.03
Random_250 × 12450N10t70_27000	27	14	275	17.02	643	1	0.00	152	0.87	643	3	0.03
Random_250 × 12450N10t70_27001	27	14	275	17.02	643	1	0.00	150	0.81	643	3	0.03
Random_250 × 12450N10t70_27002	27	14	275	17.02	643	1	0.00	152	0.84	643	3	0.03
Random_250 × 12450N10t70_27003	27	14	275	17.02	643	1	0.00	152	0.86	643	3	0.03
Random_250 × 12450N10t70_27004	27	14	275	17.02	643	1	0.00	153	0.83	643	3	0.03
Random_250 × 12450N10t70_27005	27	14	275	17.02	643	1	0.00	153	0.82	643	3	0.03
Random_250 × 12450N10t70_27006	27	14	275	17.02	643	1	0.00	153	0.83	643	3	0.03
Random_250 × 12450N10t70_27007	27	14	275	17.02	643	1	0.00	152	0.82	643	3	0.03
Random_250 × 12450N10t70_27008	27	14	275	17.02	643	1	0.00	154	0.87	643	3	0.03
Random_250 × 12450N10t70_27009	27	14	275	17.02	643	1	0.00	152	0.86	643	3	0.03
Random_250 × 12450N25t70_27000	64	9	312	13.26	2119	1	0.00	160	1.89	2119	15	0.04
Random_250 × 12450N25t70_27001	64	9	312	13.26	2119	1	0.00	151	2.01	2119	15	0.04
Random_250 × 12450N25t70_27002	64	9	312	13.26	2119	1	0.00	158	2.03	2119	15	0.04
Random_250 × 12450N25t70_27003	64	9	312	13.26	2119	1	0.00	160	2.00	2119	15	0.04
Random_250 × 12450N25t70_27004	64	9	312	13.26	2119	1	0.00	160	2.01	2119	15	0.04
Random_250 × 12450N25t70_27005	64	9	312	13.26	2119	1	0.00	158	2.05	2119	15	0.03
Random_250 × 12450N25t70_27006	64	9	312	13.26	2119	1	0.00	160	2.01	2119	15	0.03
Random_250 × 12450N25t70_27007	64	9	312	13.26	2119	1	0.00	158	2.03	2119	15	0.03
Random_250 × 12450N25t70_27008	64	9	312	13.26	2119	1	0.00	160	2.02	2119	15	0.03
Random_250 × 12450N25t70_27009	64	9	312	13.26	2119	1	0.00	158	2.06	2119	15	0.03
Random_250 × 18675N10t10_27000	27	1	275	24.89	858	1	0.00	26	0.37	858	1	0.03
Random_250 × 18675N10t10_27001	27	1	275	24.89	858	1	0.00	26	0.38	858	1	0.03
Random_250 × 18675N10t10_27002	27	1	275	24.89	858	1	0.00	26	0.40	858	1	0.03
Random_250 × 18675N10t10_27003	27	1	275	24.89	858	1	0.00	26	0.39	858	1	0.03
Random_250 × 18675N10t10_27004	27	1	275	24.89	858	1	0.00	26	0.39	858	1	0.03
Random_250 × 18675N10t10_27005	27	1	275	24.89	858	1	0.00	26	0.39	858	1	0.03
Random_250 × 18675N10t10_27006	27	1	275	24.89	858	1	0.00	26	0.38	858	1	0.03
Random_250 × 18675N10t10_27007	27	1	275	24.89	858	1	0.00	26	0.39	858	1	0.03
Random_250 × 18675N10t10_27008	27	1	275	24.89	858	1	0.00	26	0.39	858	1	0.03
Random_250 × 18675N10t10_27009	27	1	275	24.89	858	1	0.00	26	0.38	858	1	0.03
Random_250 × 18675N10t70_27000	27	12	275	25.28	548	1	0.00	126	0.95	548	1	0.03
Random_250 × 18675N10t70_27001	27	12	275	25.28	548	1	0.00	121	0.99	548	1	0.03
Random_250 × 18675N10t70_27002	27	12	275	25.28	548	1	0.00	121	1.01	548	1	0.03
Random_250 × 18675N10t70_27003	27	12	275	25.28	548	1	0.00	126	0.99	548	1	0.03
Random_250 × 18675N10t70_27004	27	12	275	25.28	548	1	0.00	119	1.01	548	1	0.03
Random_250 × 18675N10t70_27005	27	12	275	25.28	548	1	0.00	121	1.01	548	1	0.03
Random_250 × 18675N10t70_27006	27	12	275	25.28	548	1	0.00	119	1.00	548	1	0.03
Random_250 × 18675N10t70_27007	27	12	275	25.28	548	1	0.00	116	0.98	548	1	0.03
Random_250 × 18675N10t70_27008	27	12	275	25.28	548	1	0.00	118	0.90	548	1	0.03
Random_250 × 18675N10t70_27009	27	12	275	25.28	548	1	0.00	121	0.99	548	1	0.03
Random_250 × 18675N25t70_27000	64	7	312	19.67	1638	1	0.00	139	2.30	1638	1	0.03
Random_250 × 18675N25t70_27001	64	7	312	19.67	1638	1	0.00	137	2.29	1638	1	0.03
Random_250 × 18675N25t70_27002	64	7	312	19.67	1638	1	0.00	139	2.27	1638	1	0.03
Random_250 × 18675N25t70_27003	64	7	312	19.67	1638	1	0.00	137	2.35	1638	1	0.03
Random_250 × 18675N25t70_27004	64	7	312	19.67	1638	1	0.00	139	2.38	1638	1	0.03
Random_250 × 18675N25t70_27005	64	7	312	19.67	1638	1	0.00	139	2.38	1638	1	0.03
Random_250 × 18675N25t70_27006	64	7	312	19.67	1638	1	0.00	137	2.37	1638	1	0.03
Random_250 × 18675N25t70_27007	64	7	312	19.67	1638	1	0.00	137	2.29	1638	1	0.03
Random_250 × 18675N25t70_27008	64	7	312	19.67	1638	1	0.00	137	2.31	1638	1	0.03
Random_250 × 18675N25t70_27009	64	7	312	19.67	1638	1	0.00	139	2.33	1638	1	0.03
Random_250 × 24900N10t10_27000	27	1	275	33.15	846	1	0.00	26	0.50	846	1	0.03
Random_250 × 24900N10t10_27001	27	1	275	33.15	846	1	0.00	26	0.52	846	1	0.03
Random_250 × 24900N10t10_27002	27	1	275	33.15	846	1	0.00	26	0.51	846	1	0.03
Random_250 × 24900N10t10_27003	27	1	275	33.15	846	1	0.00	26	0.52	846	1	0.03
Random_250 × 24900N10t10_27004	27	1	275	33.15	846	1	0.00	26	0.51	846	1	0.03
Random_250 × 24900N10t10_27005	27	1	275	33.15	846	1	0.00	26	0.52	846	1	0.03
Random_250 × 24900N10t10_27006	27	1	275	33.15	846	1	0.00	26	0.52	846	1	0.03

(*continued on next page*)

Table 3 (*continued*).

instanceName	nbSet	maxSize	nbNodes	density	BP_value	BP_nodes	BP_gap	BP_cols	BP_cpu	BBnew_value	BBnew_nodes	BBnew_cpu
Random_250 × 24900N10t10_27007	27	1	275	33.15	846	1	0.00	26	0.52	846	1	0.03
Random_250 × 24900N10t10_27008	27	1	275	33.15	846	1	0.00	26	0.50	846	1	0.03
Random_250 × 24900N10t10_27009	27	1	275	33.15	846	1	0.00	26	0.52	846	1	0.03
Random_250 × 24900N10t70_27000	27	10	275	33.54	485	1	0.00	127	1.12	485	1	0.03
Random_250 × 24900N10t70_27001	27	10	275	33.54	485	1	0.00	127	1.12	485	1	0.03
Random_250 × 24900N10t70_27002	27	10	275	33.54	485	1	0.00	127	1.10	485	1	0.03
Random_250 × 24900N10t70_27003	27	10	275	33.54	485	1	0.00	127	1.15	485	1	0.03
Random_250 × 24900N10t70_27004	27	10	275	33.54	485	1	0.00	127	1.10	485	1	0.03
Random_250 × 24900N10t70_27005	27	10	275	33.54	485	1	0.00	127	1.17	485	1	0.03
Random_250 × 24900N10t70_27006	27	10	275	33.54	485	1	0.00	127	1.14	485	1	0.03
Random_250 × 24900N10t70_27007	27	10	275	33.54	485	1	0.00	127	1.14	485	1	0.03
Random_250 × 24900N10t70_27008	27	10	275	33.54	485	1	0.00	127	1.13	485	1	0.03
Random_250 × 24900N10t70_27009	27	10	275	33.54	485	1	0.00	119	1.01	485	1	0.03
Random_250 × 24900N25t70_27004	64	5	312	26.09	1616	1	0.00	162	2.98	1616	7	0.04
Random_250 × 24900N25t70_27005	64	5	312	26.09	1616	1	0.00	161	3.10	1616	7	0.04
Random_250 × 24900N25t70_27006	64	5	312	26.09	1616	1	0.00	160	3.07	1616	7	0.04
Random_250 × 24900N25t70_27007	64	5	312	26.09	1616	1	0.00	159	3.10	1616	7	0.04
Random_250 × 24900N25t70_27008	64	5	312	26.09	1616	1	0.00	159	3.09	1616	7	0.04
Random_250 × 24900N25t70_27009	64	5	312	26.09	1616	1	0.00	164	3.15	1616	7	0.04
Random_250 × 31125N10t70_27005	27	11	275	41.81	471	1	0.00	133	1.40	471	1	0.04
Random_250 × 31125N10t70_27006	27	11	275	41.81	471	1	0.00	121	1.42	471	1	0.04
Random_250 × 31125N10t70_27007	27	11	275	41.81	471	1	0.00	122	1.37	471	1	0.04
Random_250 × 31125N10t70_27008	27	11	275	41.81	471	1	0.00	132	1.40	471	1	0.04
Random_250 × 31125N10t70_27009	27	11	275	41.81	471	1	0.00	132	1.37	471	1	0.04
Random_250 × 31125N25t70_27000	64	8	312	32.50	1416	1	0.00	136	3.35	1416	3	0.04
Random_250 × 31125N25t70_27001	64	8	312	32.50	1416	1	0.00	134	3.31	1416	3	0.04
Random_250 × 31125N25t70_27002	64	8	312	32.50	1416	1	0.00	139	3.40	1416	3	0.04
Random_250 × 31125N25t70_27003	64	8	312	32.50	1416	1	0.00	138	3.35	1416	3	0.04
Random_250 × 31125N25t70_27004	64	8	312	32.50	1416	1	0.00	136	3.31	1416	3	0.04
Random_250 × 31125N25t70_27005	64	8	312	32.50	1416	1	0.00	140	3.47	1416	3	0.04
Random_250 × 31125N25t70_27006	64	8	312	32.50	1416	1	0.00	135	3.43	1416	3	0.04
Random_250 × 31125N25t70_27007	64	8	312	32.50	1416	1	0.00	136	3.35	1416	3	0.04
Random_250 × 31125N25t70_27008	64	8	312	32.50	1416	1	0.00	136	3.31	1416	3	0.04
Random_250 × 31125N25t70_27009	64	8	312	32.50	1416	1	0.00	132	3.38	1416	3	0.04
Random_250 × 6225N10t10_27000	27	1	275	8.36	1421	1	0.00	30	0.15	1421	7	0.03
Random_250 × 6225N10t10_27001	27	1	275	8.36	1421	1	0.00	30	0.15	1421	7	0.03
Random_250 × 6225N10t10_27002	27	1	275	8.36	1421	1	0.00	30	0.14	1421	7	0.03
Random_250 × 6225N10t10_27003	27	1	275	8.36	1421	1	0.00	30	0.15	1421	7	0.03
Random_250 × 6225N10t10_27004	27	1	275	8.36	1421	1	0.00	30	0.14	1421	7	0.03
Random_250 × 6225N10t10_27005	27	1	275	8.36	1421	1	0.00	30	0.15	1421	7	0.03
Random_250 × 6225N10t10_27006	27	1	275	8.36	1421	1	0.00	30	0.15	1421	7	0.03
Random_250 × 6225N10t10_27007	27	1	275	8.36	1421	1	0.00	30	0.14	1421	7	0.03
Random_250 × 6225N10t10_27008	27	1	275	8.36	1421	1	0.00	30	0.15	1421	7	0.03
Random_250 × 6225N10t10_27009	27	1	275	8.36	1421	1	0.00	30	0.14	1421	7	0.03
Random_250 × 6225N10t70_27000	27	13	275	8.76	875	1	0.00	128	0.55	875	1	0.03
Random_250 × 6225N10t70_27001	27	13	275	8.76	875	1	0.00	129	0.53	875	1	0.03
Random_250 × 6225N10t70_27002	27	13	275	8.76	875	1	0.00	135	0.56	875	1	0.03
Random_250 × 6225N10t70_27003	27	13	275	8.76	875	1	0.00	143	0.58	875	1	0.03
Random_250 × 6225N10t70_27004	27	13	275	8.76	875	1	0.00	118	0.52	875	1	0.03
Random_250 × 6225N10t70_27005	27	13	275	8.76	875	1	0.00	129	0.52	875	1	0.03
Random_250 × 6225N10t70_27006	27	13	275	8.76	875	1	0.00	143	0.59	875	1	0.03
Random_250 × 6225N10t70_27007	27	13	275	8.76	875	1	0.00	131	0.57	875	1	0.03
Random_250 × 6225N10t70_27008	27	13	275	8.76	875	1	0.00	134	0.56	875	1	0.03
Random_250 × 6225N10t70_27009	27	13	275	8.76	875	1	0.00	143	0.60	875	1	0.03
Random_250 × 6225N25t70_27000	64	7	312	6.84	2875	1	0.00	169	1.46	2875	261	0.07
Random_250 × 6225N25t70_27001	64	7	312	6.84	2875	1	0.00	170	1.45	2875	261	0.07
Random_250 × 6225N25t70_27002	64	7	312	6.84	2875	1	0.00	169	1.47	2875	261	0.07
Random_250 × 6225N25t70_27003	64	7	312	6.84	2875	1	0.00	171	1.50	2875	261	0.07
Random_250 × 6225N25t70_27004	64	7	312	6.84	2875	1	0.00	167	1.45	2875	261	0.07
Random_250 × 6225N25t70_27005	64	7	312	6.84	2875	1	0.00	169	1.47	2875	261	0.07
Random_250 × 6225N25t70_27006	64	7	312	6.84	2875	1	0.00	170	1.43	2875	261	0.07
Random_250 × 6225N25t70_27007	64	7	312	6.84	2875	1	0.00	171	1.45	2875	261	0.07
Random_250 × 6225N25t70_27008	64	7	312	6.84	2875	1	0.00	170	1.40	2875	261	0.07
Random_250 × 6225N25t70_27009	64	7	312	6.84	2875	1	0.00	169	1.42	2875	261	0.07
Random_500 × 24950N10t10_27000	52	1	550	8.31	2280	1	0.00	55	1.37	2280	7	0.21
Random_500 × 24950N10t10_27001	52	1	550	8.31	2280	1	0.00	55	1.34	2280	7	0.21
Random_500 × 24950N10t10_27002	52	1	550	8.31	2280	1	0.00	55	1.36	2280	7	0.21
Random_500 × 24950N10t10_27003	52	1	550	8.31	2280	1	0.00	55	1.38	2280	7	0.21
Random_500 × 24950N10t10_27004	52	1	550	8.31	2280	1	0.00	55	1.39	2280	7	0.21
Random_500 × 24950N10t10_27005	52	1	550	8.31	2280	1	0.00	55	1.37	2280	7	0.21
Random_500 × 24950N10t10_27006	52	1	550	8.31	2280	1	0.00	55	1.36	2280	7	0.21
Random_500 × 24950N10t10_27007	52	1	550	8.31	2280	1	0.00	55	1.35	2280	7	0.21
Random_500 × 24950N10t10_27008	52	1	550	8.31	2280	1	0.00	55	1.37	2280	7	0.21
Random_500 × 24950N10t10_27009	52	1	550	8.31	2280	1	0.00	55	1.36	2280	7	0.21

(*continued on next page*)

Table 3 (*continued*).

instanceName	nbSet	maxSize	nbNodes	density	BP_value	BP_nodes	BP_gap	BP_cols	BP_cpu	BBnew_value	BBnew_nodes	BBnew_cpu
Random_500 × 24950N10t70_27000	52	12	550	8.51	1443	1	0.00	277	4.82	1443	7	0.22
Random_500 × 24950N10t70_27001	52	12	550	8.51	1443	1	0.00	262	4.84	1443	7	0.22
Random_500 × 24950N10t70_27002	52	12	550	8.51	1443	1	0.00	277	4.84	1443	7	0.22
Random_500 × 24950N10t70_27003	52	12	550	8.51	1443	1	0.00	269	4.80	1443	7	0.22
Random_500 × 24950N10t70_27004	52	12	550	8.51	1443	1	0.00	277	4.75	1443	7	0.22
Random_500 × 24950N10t70_27005	52	12	550	8.51	1443	1	0.00	277	4.88	1443	7	0.22
Random_500 × 24950N10t70_27006	52	12	550	8.51	1443	1	0.00	277	4.86	1443	7	0.22
Random_500 × 24950N10t70_27007	52	12	550	8.51	1443	1	0.00	269	4.80	1443	7	0.22
Random_500 × 24950N10t70_27008	52	12	550	8.51	1443	1	0.00	277	4.84	1443	7	0.22
Random_500 × 24950N10t70_27009	52	12	550	8.51	1443	1	0.00	262	4.77	1443	7	0.22
Random_500 × 24950N25t70_27000	127	6	625	6.61	4687	1	0.00	352	14.70	4687	3013	2.36
Random_500 × 24950N25t70_27001	127	6	625	6.61	4687	1	0.00	354	15.01	4687	3013	2.37
Random_500 × 24950N25t70_27002	127	6	625	6.61	4687	1	0.00	351	14.69	4687	3013	2.39
Random_500 × 24950N25t70_27003	127	6	625	6.61	4687	1	0.00	329	14.88	4687	3013	2.35
Random_500 × 24950N25t70_27004	127	6	625	6.61	4687	1	0.00	352	14.70	4687	3013	2.31
Random_500 × 24950N25t70_27005	127	6	625	6.61	4687	1	0.00	345	14.93	4687	3013	2.31
Random_500 × 24950N25t70_27006	127	6	625	6.61	4687	1	0.00	350	14.64	4687	3013	2.30
Random_500 × 24950N25t70_27007	127	6	625	6.61	4687	1	0.00	353	14.85	4687	3013	2.31
Random_500 × 24950N25t70_27008	127	6	625	6.61	4687	1	0.00	333	14.61	4687	3013	2.30
Random_500 × 24950N25t70_27009	127	6	625	6.61	4687	1	0.00	340	14.94	4687	3013	2.30
Random_500 × 49900N10t10_27000	52	1	550	16.58	1750	1	0.00	51	2.46	1750	1	0.22
Random_500 × 49900N10t10_27001	52	1	550	16.58	1750	1	0.00	51	2.46	1750	1	0.22
Random_500 × 49900N10t10_27002	52	1	550	16.58	1750	1	0.00	51	2.49	1750	1	0.22
Random_500 × 49900N10t10_27003	52	1	550	16.58	1750	1	0.00	51	2.46	1750	1	0.22
Random_500 × 49900N10t10_27004	52	1	550	16.58	1750	1	0.00	51	2.46	1750	1	0.22
Random_500 × 49900N10t10_27005	52	1	550	16.58	1750	1	0.00	51	2.45	1750	1	0.22
Random_500 × 49900N10t10_27006	52	1	550	16.58	1750	1	0.00	51	2.45	1750	1	0.22
Random_500 × 49900N10t10_27007	52	1	550	16.58	1750	1	0.00	51	2.43	1750	1	0.22
Random_500 × 49900N10t10_27008	52	1	550	16.58	1750	1	0.00	51	2.48	1750	1	0.22
Random_500 × 49900N10t10_27009	52	1	550	16.58	1750	1	0.00	51	2.44	1750	1	0.22
Random_500 × 49900N10t70_27000	52	14	550	16.77	1136	1	0.00	248	6.48	1136	3	0.23
Random_500 × 49900N10t70_27001	52	14	550	16.77	1136	1	0.00	248	6.59	1136	3	0.23
Random_500 × 49900N10t70_27002	52	14	550	16.77	1136	1	0.00	254	6.48	1136	3	0.23
Random_500 × 49900N10t70_27003	52	14	550	16.77	1136	1	0.00	248	6.54	1136	3	0.23
Random_500 × 49900N10t70_27004	52	14	550	16.77	1136	1	0.00	248	6.45	1136	3	0.23
Random_500 × 49900N10t70_27005	52	14	550	16.77	1136	1	0.00	243	6.45	1136	3	0.23
Random_500 × 49900N10t70_27006	52	14	550	16.77	1136	1	0.00	261	6.55	1136	3	0.23
Random_500 × 49900N10t70_27007	52	14	550	16.77	1136	1	0.00	250	6.70	1136	3	0.23
Random_500 × 49900N10t70_27008	52	14	550	16.77	1136	1	0.00	243	6.53	1136	3	0.23
Random_500 × 49900N10t70_27009	52	14	550	16.77	1136	1	0.00	243	6.53	1136	3	0.23
Random_500 × 49900N25t70_27000	127	8	625	13.01	3632	1	0.00	291	20.00	3632	35	0.25
Random_500 × 49900N25t70_27001	127	8	625	13.01	3632	1	0.00	293	19.80	3632	35	0.25
Random_500 × 49900N25t70_27002	127	8	625	13.01	3632	1	0.00	292	19.73	3632	35	0.25
Random_500 × 49900N25t70_27003	127	8	625	13.01	3632	1	0.00	294	20.03	3632	35	0.25
Random_500 × 49900N25t70_27004	127	8	625	13.01	3632	1	0.00	292	19.92	3632	35	0.25
Random_500 × 49900N25t70_27005	127	8	625	13.01	3632	1	0.00	295	20.04	3632	35	0.25
Random_500 × 49900N25t70_27006	127	8	625	13.01	3632	1	0.00	292	19.70	3632	35	0.24
Random_500 × 49900N25t70_27007	127	8	625	13.01	3632	1	0.00	291	19.60	3632	35	0.24
Random_500 × 49900N25t70_27008	127	8	625	13.01	3632	1	0.00	292	20.12	3632	35	0.25
Random_500 × 49900N25t70_27009	127	8	625	13.01	3632	1	0.00	296	20.06	3632	35	0.25
Random_500 × 74850N10t10_27000	52	1	550	24.84	1576	1	0.00	51	3.80	1576	1	0.23
Random_500 × 74850N10t10_27001	52	1	550	24.84	1576	1	0.00	51	3.82	1576	1	0.23
Random_500 × 74850N10t10_27002	52	1	550	24.84	1576	1	0.00	51	3.84	1576	1	0.23
Random_500 × 74850N10t10_27003	52	1	550	24.84	1576	1	0.00	51	3.69	1576	1	0.23
Random_500 × 74850N10t10_27004	52	1	550	24.84	1576	1	0.00	51	3.81	1576	1	0.23
Random_500 × 74850N10t10_27005	52	1	550	24.84	1576	1	0.00	51	3.75	1576	1	0.23
Random_500 × 74850N10t10_27006	52	1	550	24.84	1576	1	0.00	51	3.74	1576	1	0.23
Random_500 × 74850N10t10_27007	52	1	550	24.84	1576	1	0.00	51	3.85	1576	1	0.23
Random_500 × 74850N10t10_27008	52	1	550	24.84	1576	1	0.00	51	3.79	1576	1	0.23
Random_500 × 74850N10t10_27009	52	1	550	24.84	1576	1	0.00	51	3.70	1576	1	0.23
Random_500 × 74850N10t70_27000	52	13	550	25.04	1030	1	0.00	241	8.32	1030	1	0.23
Random_500 × 74850N10t70_27001	52	13	550	25.04	1030	1	0.00	250	8.99	1030	1	0.23
Random_500 × 74850N10t70_27002	52	13	550	25.04	1030	1	0.00	242	8.32	1030	1	0.23
Random_500 × 74850N10t70_27003	52	13	550	25.04	1030	1	0.00	251	8.23	1030	1	0.23
Random_500 × 74850N10t70_27004	52	13	550	25.04	1030	1	0.00	242	8.85	1030	1	0.23
Random_500 × 74850N10t70_27005	52	13	550	25.04	1030	1	0.00	242	8.53	1030	1	0.23
Random_500 × 74850N10t70_27006	52	13	550	25.04	1030	1	0.00	242	8.41	1030	1	0.23
Random_500 × 74850N10t70_27007	52	13	550	25.04	1030	1	0.00	255	8.46	1030	1	0.23
Random_500 × 74850N10t70_27008	52	13	550	25.04	1030	1	0.00	263	8.49	1030	1	0.23
Random_500 × 74850N10t70_27009	52	13	550	25.04	1030	1	0.00	242	8.31	1030	1	0.23
Random_500 × 74850N25t70_27000	127	6	625	19.40	3134	1	0.00	281	25.49	3134	3	0.23
Random_500 × 74850N25t70_27001	127	6	625	19.40	3134	1	0.00	280	24.53	3134	3	0.23
Random_500 × 74850N25t70_27002	127	6	625	19.40	3134	1	0.00	281	24.96	3134	3	0.23
Random_500 × 74850N25t70_27003	127	6	625	19.40	3134	1	0.00	284	24.42	3134	3	0.23
Random_500 × 74850N25t70_27004	127	6	625	19.40	3134	1	0.00	279	24.84	3134	3	0.23
Random_500 × 74850N25t70_27005	127	6	625	19.40	3134	1	0.00	283	24.57	3134	3	0.23

(*continued on next page*)

Table 3 (*continued*).

instanceName	nbSet	maxSize	nbNodes	density	BP_value	BP_nodes	BP_gap	BP_cols	BP_cpu	BBnew_value	BBnew_nodes	BBnew_cpu
Random_500 × 74850N25t70_27006	127	6	625	19.40	3134	1	0.00	283	25.16	3134	3	0.23
Random_500 × 74850N25t70_27007	127	6	625	19.40	3134	1	0.00	276	25.32	3134	3	0.23
Random_500 × 74850N25t70_27008	127	6	625	19.40	3134	1	0.00	284	25.59	3134	3	0.23
Random_500 × 74850N25t70_27009	127	6	625	19.40	3134	1	0.00	284	24.33	3134	3	0.23
Random_500 × 99800N10t10_27000	52	1	550	33.10	1509	1	0.00	51	5.19	1509	1	0.24
Random_500 × 99800N10t10_27001	52	1	550	33.10	1509	1	0.00	51	5.09	1509	1	0.24
Random_500 × 99800N10t10_27002	52	1	550	33.10	1509	1	0.00	51	5.19	1509	1	0.24
Random_500 × 99800N10t10_27003	52	1	550	33.10	1509	1	0.00	51	5.00	1509	1	0.24
Random_500 × 99800N10t10_27004	52	1	550	33.10	1509	1	0.00	51	5.04	1509	1	0.24
Random_500 × 99800N10t10_27005	52	1	550	33.10	1509	1	0.00	51	5.16	1509	1	0.24
Random_500 × 99800N10t10_27006	52	1	550	33.10	1509	1	0.00	51	5.44	1509	1	0.24
Random_500 × 99800N10t10_27007	52	1	550	33.10	1509	1	0.00	51	5.00	1509	1	0.24
Random_500 × 99800N10t10_27008	52	1	550	33.10	1509	1	0.00	51	5.19	1509	1	0.24
Random_500 × 99800N10t10_27009	52	1	550	33.10	1509	1	0.00	51	5.19	1509	1	0.24
Random_500 × 99800N10t70_27000	52	15	550	33.30	933	1	0.00	203	9.85	933	1	0.24
Random_500 × 99800N10t70_27001	52	15	550	33.30	933	1	0.00	208	9.99	933	1	0.24
Random_500 × 99800N10t70_27002	52	15	550	33.30	933	1	0.00	203	10.49	933	1	0.24
Random_500 × 99800N10t70_27003	52	15	550	33.30	933	1	0.00	203	10.08	933	1	0.24
Random_500 × 99800N10t70_27004	52	15	550	33.30	933	1	0.00	203	10.35	933	1	0.24
Random_500 × 99800N10t70_27005	52	15	550	33.30	933	1	0.00	203	9.84	933	1	0.24
Random_500 × 99800N10t70_27006	52	15	550	33.30	933	1	0.00	208	9.65	933	1	0.24
Random_500 × 99800N10t70_27007	52	15	550	33.30	933	1	0.00	203	10.19	933	1	0.24
Random_500 × 99800N10t70_27008	52	15	550	33.30	933	1	0.00	203	10.13	933	1	0.24
Random_500 × 99800N10t70_27009	52	15	550	33.30	933	1	0.00	203	9.56	933	1	0.24
Random_500 × 99800N25t70_27000	127	7	625	25.80	2969	1	0.00	315	33.78	2969	1	0.24
Random_500 × 99800N25t70_27001	127	7	625	25.80	2969	1	0.00	320	33.63	2969	1	0.24
Random_500 × 99800N25t70_27002	127	7	625	25.80	2969	1	0.00	316	31.74	2969	1	0.24
Random_500 × 99800N25t70_27003	127	7	625	25.80	2969	1	0.00	315	33.52	2969	1	0.24
Random_500 × 99800N25t70_27004	127	7	625	25.80	2969	1	0.00	314	33.47	2969	1	0.24
Random_500 × 99800N25t70_27005	127	7	625	25.80	2969	1	0.00	322	31.98	2969	1	0.24
Random_500 × 99800N25t70_27006	127	7	625	25.80	2969	1	0.00	313	32.08	2969	1	0.24
Random_500 × 99800N25t70_27007	127	7	625	25.80	2969	1	0.00	318	32.12	2969	1	0.24
Random_500 × 99800N25t70_27008	127	7	625	25.80	2969	1	0.00	316	32.02	2969	1	0.24
Random_500 × 99800N25t70_27009	127	7	625	25.80	2969	1	0.00	318	33.03	2969	1	0.24

CRediT authorship contribution statement

Sébastien Martin: Methodology, Software, Supervision, Writing – review & editing. **Youcef Magnouche:** Software, Supervision, Visualization, Writing – review & editing. **Corentin Juvigny:** Methodology, Investigation, Software, Writing – original draft. **Jérémie Leguay:** Conceptualization, Investigation, Validation, Writing – review & editing.

Acknowledgments

We would like to thank Daniele Ferone for providing the $B\&B^{new}$ executable and the Literature instances.

Appendix

In the following you can find all the numerical results presented in figures. In Tables 1–3, we have the following entries

- instanceName : the name of the instance.
- nbSet : the number of inclusion subsets.
- maxSize : the maximum size of inclusions subsets.
- nbNodes : the number of nodes after the graph transformation.
- density : the density of the network after the graph transformation.
- BP_value : the objective value given by the Branch-and-Price algorithm.
- BP_nodes : the number of nodes in the branching tree of the Branch-and-Price algorithm.
- BP_gap : the relative error between the best upper and lower bound obtained at the root node of the branching tree.
- BP_cols : the total number of columns generated by in the Branch-and-Price algorithm.
- BP_cpu : the cpu time associated with the Branch-and-Price algorithm.
- BBnew_value : the objective value given by BBnew algorithm.
- BBnew_nodes : the number of nodes in the branching tree of BBnew algorithm.
- BBnew_cpu : the cpu time associated with BBnew algorithm.

References

de Andrade, R.C., Saraiva, R.D., 2018. An integer linear programming model for the constrained shortest path tour problem. Electron. Notes Discrete Math. 69, 141–148.

Barnhart, C., Hane, C.A., Vance, P.H., 2000. Using branch-and-price-and-cut to solve origin-destination integer multicommodity flow problems. Oper. Res. 48 (2), 318–326.

Bertossi, A.A., 1981. The edge Hamiltonian path problem is NP-complete. Inform. Process. Lett. 13 (4–5), 157–159.

Bhamare, D., Jain, R., Samaka, M., Erbad, A., 2016a. A survey on service function chaining. J. Netw. Comput. Appl. 75, 138–155.

Bhamare, D., Jain, R., Samaka, M., Erbad, A., 2016b. A survey on service function chaining. J. Netw. Comput. Appl. 75, 138–155.

Carrabs, F., D'Ambrosio, C., Ferone, D., Festa, P., Laureana, F., 2020. The constrained forward shortest path tour problem: Mathematical modeling and GRASP approximate solutions. Networks 17–31.

Dantzig, G.B., Wolfe, P., 1960. Decomposition principle for linear programs. Oper. Res. 8 (1), 101–111.

Dezs, B., Jüttner, A., Kovács, P., 2011. Lemon - an open source c++ graph template library. Electron. Notes Theor. Comput. Sci. 264 (5), 23–45.

Di Puglia Pugliese, L., Ferone, D., Festa, P., Guerriero, F., 2020. Shortest path tour problem with time windows. European J. Oper. Res. 282 (1), 334–344. http://dx.doi.org/10.1016/j.ejor.2019.08.052, URL https://www.sciencedirect.com/science/article/pii/S0377221719307222.

Dwaraki, A., Wolf, T., 2016. Adaptive service-chain routing for virtual network functions in software-defined networks. In: Proceedings of the 2016 workshop on Hot topics in Middleboxes and Network Function Virtualization. Association for Computing Machinery, pp. 32–37.

Escudero, L.F., Guignard, M., Malik, K., 1994. A lagrangian relax-and-cut approach for the sequential ordering problem with precedence relationships. European J. Oper. Res. 219–237.

Ferone, D., Festa, P., Guerriero, F., 2020. An efficient exact approach for the constrained shortest path tour problem. Optim. Methods Softw. 35 (1), 1–20.

Ferone, D., Festa, P., Guerriero, F., Laganà, D., 2016. The constrained shortest path tour problem. Comput. Oper. Res. 74, 64–77.

Festa, P., Guerriero, F., Laganà, D., Musmanno, R., 2013. Solving the shortest path tour problem. European J. Oper. Res. 230 (3), 464–474.

Garey, M.R., Johnson, D.S., 1979. Computers and Intractability, Vol. 174. freeman San Francisco.

Huin, N., Leguay, J., Martin, S., Medagliani, P., Cai, S., 2019. Routing and slot allocation in 5G hard slicing. In: INOC. pp. 72–77.

IBM, 2013. ILOG CPLEX Solver. URL https://www.ibm.com/analytics/cplex-optimizer.

Mijumbi, R., Serrat, J., Gorricho, J.-L., Latre, S., Charalambides, M., Lopez, D., 2016. Management and orchestration challenges in network functions virtualization. IEEE Commun. Mag. 54 (1), 98–105.

Montemanni, L.R., Smith, D.H., Gambardella, L.M., 2008. A heuristic manipulation technique for the sequential ordering problem. European J. Oper. Res. 3931–3944.

Saraiva, R.D., de Andrade, R.C., 2021. Constrained shortest path tour problem: models, valid inequalities, and Lagrangian heuristics. Int. Trans. Oper. Res. 28 (1), 222–261.

Sasabe, M., Hara, T., 2021. Capacitated shortest path tour problem-based integer linear programming for service chaining and function placement in NFV networks. IEEE Trans. Netw. Serv. Manag. 18 (1), 104–117. http://dx.doi.org/10.1109/TNSM.2020.3044329.

Taccari, L., 2016. Integer programming formulations for the elementary shortest path problem. European J. Oper. Res. 122–130.